REACTOR VESSEL MATERIAL SURVEILLANCE PROGRAM FOR INDIAN POINT UNIT NO. 2 ANALYSIS OF CAPSULE Y

by

E. B. Norris

FINAL REPORT

SwRI Project No. 02-5212

REGULATORY DOCKET FILE COPY

— NOTICE —

THE ATTACHED FILES ARE OFFICIAL RECORDS OF THE DIVISION OF DOCUMENT CONTROL. THEY HAVE BEEN CHARGED TO YOU FOR A LIMITED TIME PERIOD AND MUST BE RETURNED TO THE RECORDS FACILITY BRANCH 016. PLEASE DO NOT SEND DOCUMENTS CHARGED OUT THROUGH THE MAIL. REMOVAL OF ANY PAGE(S) FROM DOCUMENT FOR REPRODUCTION MUST BE REFERRED TO FILE PERSONNEL.

DEADLINE RETURN DATE ______

RECORDS FACILITY BRANCH

SOUTHWEST RESEARCH INSTITUTE

SAN ANTONIO — HOUSTON

8205120287 820505
PDR ADOCK 05000247
P PDR

Docket # 50-247
Control # 8205120270
Date 05-05-82 of Document:
REGULATORY DOCKET FILE

SOUTHWEST RESEARCH INSTITUTE
Post Office Drawer 28510, 6220 Culebra Road
San Antonio, Texas 78284

REACTOR VESSEL MATERIAL SURVEILLANCE PROGRAM FOR INDIAN POINT UNIT NO. 2 ANALYSIS OF CAPSULE Y

by

E. B. Norris

FINAL REPORT
SwRI Project No. 02-5212

Prepared for
Consolidated Edison Company of New York, Inc.
4 Irving Place
New York, New York 10003

November 1980

Approved:

U. S. Lindholm, Director
Department of Materials Sciences

REGULATORY DOCKET FILE COPY

ABSTRACT

The second vessel material surveillance capsule removed from the Indian Point Unit No. 2 nuclear power plant has been tested, and the results have been evaluated. Heatup and cooldown limit curves for normal operation have been developed for up to 5 and from 5 to 7 effective full power years of operation.

TABLE OF CONTENTS

LIST OF TABLES

LIST OF FIGURES

I. SUMMARY OF RESULTS AND CONCLUSIONS

The analysis of the second material surveillance capsule removed from the Indian Point Unit 2 reactor pressure vessel led to the following conclusions:

(1) Based on a calculated neutron spectral distribution, Capsule Y received an average fast fluence of 5.3×10^{18} cm^{-2} ($E > 1$ MeV).

(2) The surveillance specimens of the three core beltline materials experienced shifts in transition temperature of 170°F to 225°F as a result of the service exposure.

(3) The weld metal exhibited the largest shift in RT_{NDT}, but the plate material will control the heatup and cooldown limitations because of its much higher initial RT_{NDT}.

(4) The estimated maximum neutron fluence of 1.5×10^{13} cm^{-2} ($E > 1$ MeV) received by the vessel wall accrued in 2.34 full power years. Therefore, the projected maximum neutron fluence after 32 effective full power years (EFPY) is 2.1×10^{19} cm^{-2} ($E > 1$ MeV). This estimate is based on an average lead factor of 3.52 (ratio of average Capsule Y specimen flux and the maximum pressure vessel flux, $E > 1.0$ MeV).

(5) Based on Regulatory Guide 1.99 trend curves, the projected maximum RT_{NDT} for the Indian Point Unit 2 vessel core beltline materials at the 1/4T and 3/4T positions after 5 EFPY of operation are 170°F and 115°F, respectively. These values, which are consistent with the results from the analysis of Capsule T[(1)*], were used as the bases for computing heatup and cooldown limit curves for up to 5 EFPY of operation.

---

* Superscript numbers refer to references at the end of the text.

(6) Based on Regulatory Guide 1.99 trend curves, the projected maximum RT_{NDT} for the Indian Point Unit No. 2 vessel core beltline materials at the 1/4T and 3/4T positions after 7 EFPY of operation are 190°F and 125°F, respectively. These values were used as the bases for computing heatup and cooldown limit curves to be used from 5 to 7 EFPY of operation.

(7) The maximum RT_{NDT} for the Indian Point Unit 2 vessel core beltline materials at the 1/4T and 3/4T positions after 32 EFPY of operation are projected to be 340°F and 200°F, respectively.

(8) The Indian Point Unit 2 vessel plates located in the core beltline region are projected to retain sufficient toughness at the 1/4T and 3/4T positions to meet the current minimum C_v shelf energy requirements of 10CFR50 Appendix G for at least 17 EFPY of operation.

II. BACKGROUND

The allowable loadings on nuclear pressure vessels are determined by applying the rules in Appendix G, "Fracture Toughness Requirements," of 10CFR50.[2] In the case of pressure-retaining components made of ferritic materials, the allowable loadings depend on the reference stress intensity factor (K_{IR}) curve indexed to the reference nil ductility temperature (RT_{NDT}) presented in Appendix G, "Protection Against Non-ductile Failure," of Section III of the ASME Code.[3] Further, the materials in the beltline region of the reactor vessel must be monitored for radiation-induced changes in RT_{NDT} per the requirements of Appendix H, "Reactor Vessel Material Surveillance Program Requirements," of 10CFR50.

The RT_{NDT} is defined in paragraph NB-2331 of Section III of the ASME Code as the highest of the following temperatures:

(1) Drop-weight Nil Ductility Temperature (DW-NDT) per ASTM E 208;[4]

(2) 60 deg F below the 50 ft-lb Charpy V-notch (C_V) temperature;

(3) 60 deg F below the 35 mil C_V temperature.

The RT_{NDT} must be established for all materials, including weld metal and heat affected zone (HAZ) material as well as base plates and forgings, which comprise the reactor coolant pressure boundary.

It is well established that ferritic materials undergo an increase in strength and hardness and a decrease in ductility and toughness when exposed to neutron fluences in excess of 10^{17} neutrons per cm^2 ($E > 1$ MeV).[5] Also, it has been established that tramp elements, particularly copper and phosphorous, affect the radiation embrittlement response of ferritic materials.[6-8] The relationship between increase in RT_{NDT} and copper content is not defined completely. For example, Regulatory Guide 1.99, originally issued in July 1975, and revised in April 1977[8], proposes an adjustment to RT_{NDT} proportional to the square root of the neutron fluence. Westinghouse Electric Corporation, in their comments on the 1975 issue of Regulatory Guide 1.99[9], believed that the proposed relationship overestimates the shift at fluences greater than 1.9×10^{19} and underestimates the shift at fluences less than 1.9×10^{19}. On the other hand, Combustion Engineering, in their comments on the 1975 issue of Regulatory Guide 1.99[10], suggested that the proposed relationship is overly conservative at fluences below 10^{19} neutrons per cm^2 ($E > 1$ MeV). There is also disagreement concerning the prediction of C_v upper shelf response to exposure to neutron irradiation.[8-10] After reviewing the comments and evaluating additonal surveillance program data, the NRC issued a revision to Regulatory Guide 1.99 which raised the upper limit of the transition temperature adjustment curve. In this report, estimates of shifts in RT_{NDT} are based on Regulatory Guide 1.99, Revision 1.[8]

In general, the only ferritic pressure boundary materials in a nuclear plant which are expected to receive a fluence sufficient to affect RT_{NDT} are those materials which are located in the core beltline region of the reactor pressure vessel. Therefore, material surveillance programs include specimens machined from the plate or forging material and weldments which are located in such a region of high netron flux density. ASTM E 185[11] describes the current recommended practice for monitoring and evaluating the radiation-induced changes occurring in the mechanical properties of pressure vessel beltline materials.

Westinghouse has provided such a surveillance program for the Indian Point Unit No. 2 nuclear power plant. The encapsulated C_v specimens are located on the O.D. surface of the thermal shield where the fast neutron flux density is about three times that at the adjacent vessel wall surface. Therefore, the increases (shifts) in transition temperatures of the materials in the pressure vessel are generally less than the corresponding shifts observed in the surveillance specimens. However, because of azimuthal variations in neutron flux density, capsule fluences may lead or lag the maximum vessel fluence in a corresponding exposure period. For example, Capsule Y (removed during the 1978 refuelling outage) was exposed to a neutron fluence between three and four times that at the maximum exposure point on the vessel I.D., while Capsule V (scheduled for removal at a later date) is receiving a nuetron flux somewhat less than that at the point of maximum vessel exposure. The capsules also contain several dosimeter materials for experimentally determining the average neutron flux density at each capsule location during the exposure period.

The Indian Point Unit No. 2 material surveillance capsules also include tensile specimens as recommended by ASTM E 185. At the present time, irradiated tensile properties are used only to indicate that the materials tested continue to meet the requirements of the appropriate material specification. In addition, the material surveillance capsules contain wedge opening loading (WOL) fracture mechanics specimens. Current technology limits the testing of these specimens at temperatures well below the minimum service temperature to obtain valid fracture mechanics data per ASTM E 399[12], "Standard Method of Test for Plane-Strain Fracture Toughness of Metallic Materials." However, recent work reported by Mager and Witt[13] may lead to methods for evaluating high-toughness materials with small fracture mechanics specimens. Currently, the NRC suggests storing these specimens until an acceptable testing procedure has been defined.

This report describes the results obtained from testing the contents of Capsule Y. These data are analyzed to estimate the radiation-induced changes in the mechanical properties of the pressure vessel at the time of the 1978 refuelling outage as well as predicting the changes expected to occur at selected times in the future operation of the Indian Point Unit No. 2 power plant.

III. DESCRIPTION OF MATERIAL SURVEILLANCE PROGRAM

The Indian Point Unit No. 2 material surveillance program is described in detail in WCAP 7323[14], dated May 1969. Eight materials surveillance capsules (five Type I and three Type II) were placed in the reactor vessel between the thermal shield and the vessel wall prior to startup, see Figure 1. The vertical center of each capsule is opposite the vertical center of the core. The Capsule Y lead factor varies from 3.90 at the core-side layer to 3.14 at the vessel-side layer (average of 3.52).[15] The Type I capsules each contain Charpy V-notch, tensile and WOL specimens machined from the three SA533 Gr B plates located at the core beltline plus Charpy V-notch specimens machined from a reference heat of steel utilized in a number of Westinghouse surveillance programs. The Type II capsules include specimens machined from weld metal and HAZ material representative of those materials in the core beltline region of the vessel as well as base plate material. Capsule Y, one of the Type II capsules, was removed during the 1978 refuelling outage.

The chemistries and heat treatments of the vessel surveillance materials contained in Capsule Y are summarized in Table I. All test specimens were machined from each of the materials at the quarter-thickness (1/4T) location. The base metal C_V specimens were oriented with their long axis parallel to the primary rolling direction of the plate with the base of the notch perpendicular to the major plate surfaces. Tensile specimens were machined with the longitudinal axis parallel to the primary rolling direction of the plate. The WOL specimens were machined with the simulated crack perpendicular to the primary rolling direction and the major surfaces

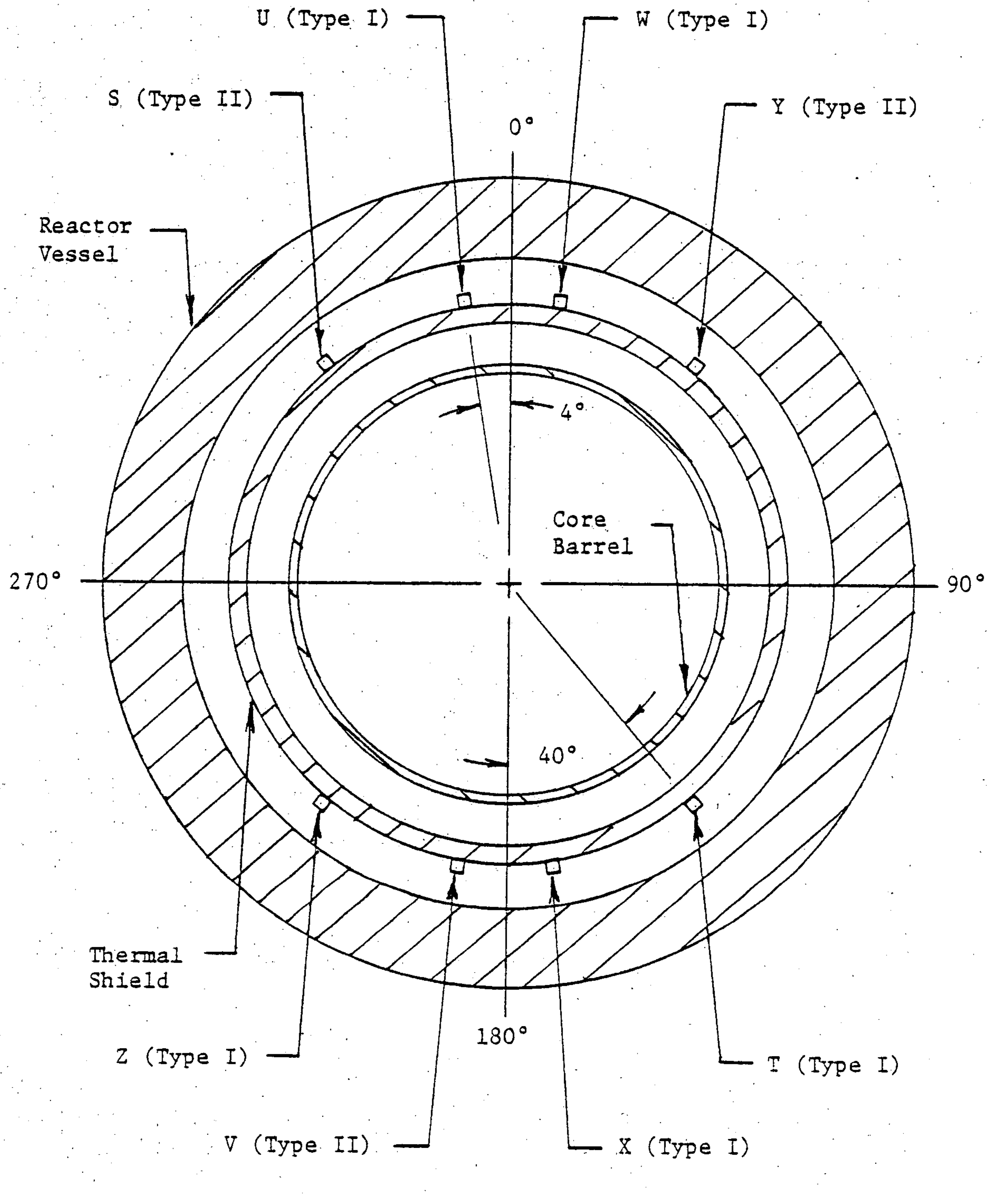

FIGURE 1. ARRANGEMENT OF SURVEILLANCE CAPSULES IN THE PRESSURE VESSEL

TABLE I

INDIAN POINT UNIT NO. 2 REACTOR VESSEL SURVEILLANCE MATERIALS(14)

Heat Treatment History

Shell Plate Material:

1550° - 1600°F, 4 hours, water quenched
1225° ± 25°F, 4 hours, air cooled
1150° ± 25°F, 40 hours, furnace cooled to 600°F

Weldment:

1150° ± 25°F, 19.75 hours, furnace cooled to 600°F

Correlation Monitor:

1650°F, 4 hours, water quenched to 300°F
1200°F, 6 hours, air cooled

Chemical Composition (Percent)

Material	C	Mn	P	S	Si	Ni	Mo	Cu
Plate B2002-1	0.20	1.28	0.010	0.019	0.25	0.58	0.46	0.25
Plate B2002-2	0.22	1.30	0.014	0.018	0.22	0.46	0.50	0.14
Plate B2002-3	0.22	1.29	0.011	0.020	0.25	0.57	0.46	0.14
Corr. Monitor	0.24	1.34	0.011	0.023	0.23	(a)	0.51	(a)
Weld Metal	(a)	(a)	(a)	(a)	(a)	(a)	(a)	(a)

(a) Not reported.

of the plate. All mechanical test specimens, see Figure 2, were taken at least one plate thickness from the quenched edges of the plate material.

Capsule Y contained 32 Charpy V-notch specimens (8 each from one of the three core beltline plates, 8 from the weld metal, 8 from the HAZ material, plus 8 from the reference steel plate); 4 tensile specimens (2 each plate and weld); and 4 WOL specimens (2 each plate and weld). The specimen numbering system and location within Capsule Y is shown in Figure 3.

Capsule Y also was reported to contain the following dosimeters for determining the neutron flux density:

Target Element	Form	Quantity
Copper	Bare wire	2
Nickel	Bare wire	1
Cobalt (in aluminum)	Bare wire	3
Cobalt (in aluminum)	Cd shielded wire	3
Uranium-238	Cd shielded wire	1
Neptunium-237	Cd shielded wire	1

In addition, corners were cut from ten C_v specimens to serve as iron dosimeters.

Three eutectic alloy thermal monitors had been inserted in holes in the steel spacers in Capsule Y. Two (located top and bottom) were 2.5% Ag and 97.5% Pb with a melting point of 579°F. The third (located at the center of the capsule) was 1.75% Ag, 0.75% Sn, and 97.5% Pb having a melting point of 590°F.

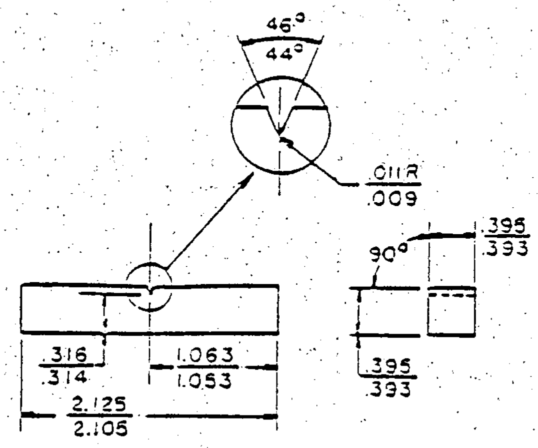

(a) Charpy V-Notch Impact Specimen

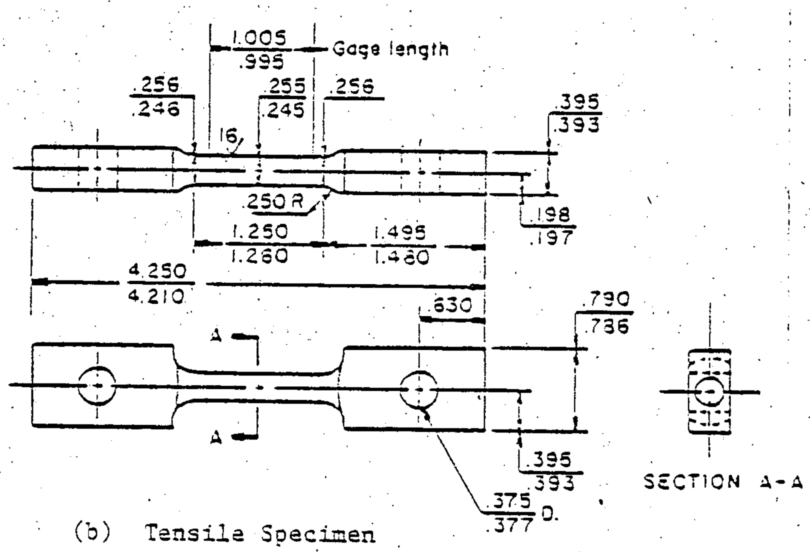

(b) Tensile Specimen

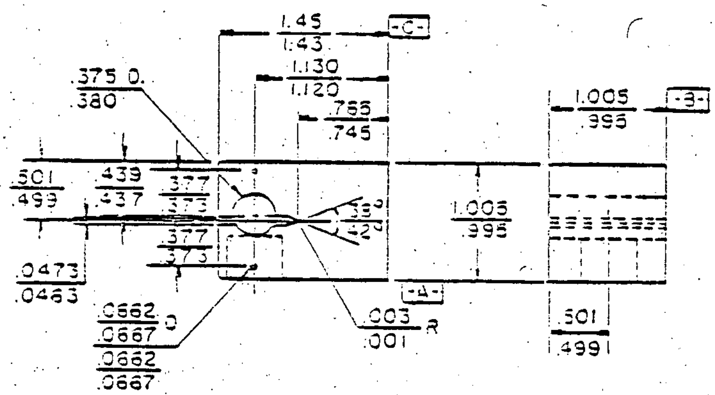

(c) Wedge Opening Loading Specimen

FIGURE 2. VESSEL MATERIAL SURVEILLANCE SPECIMENS

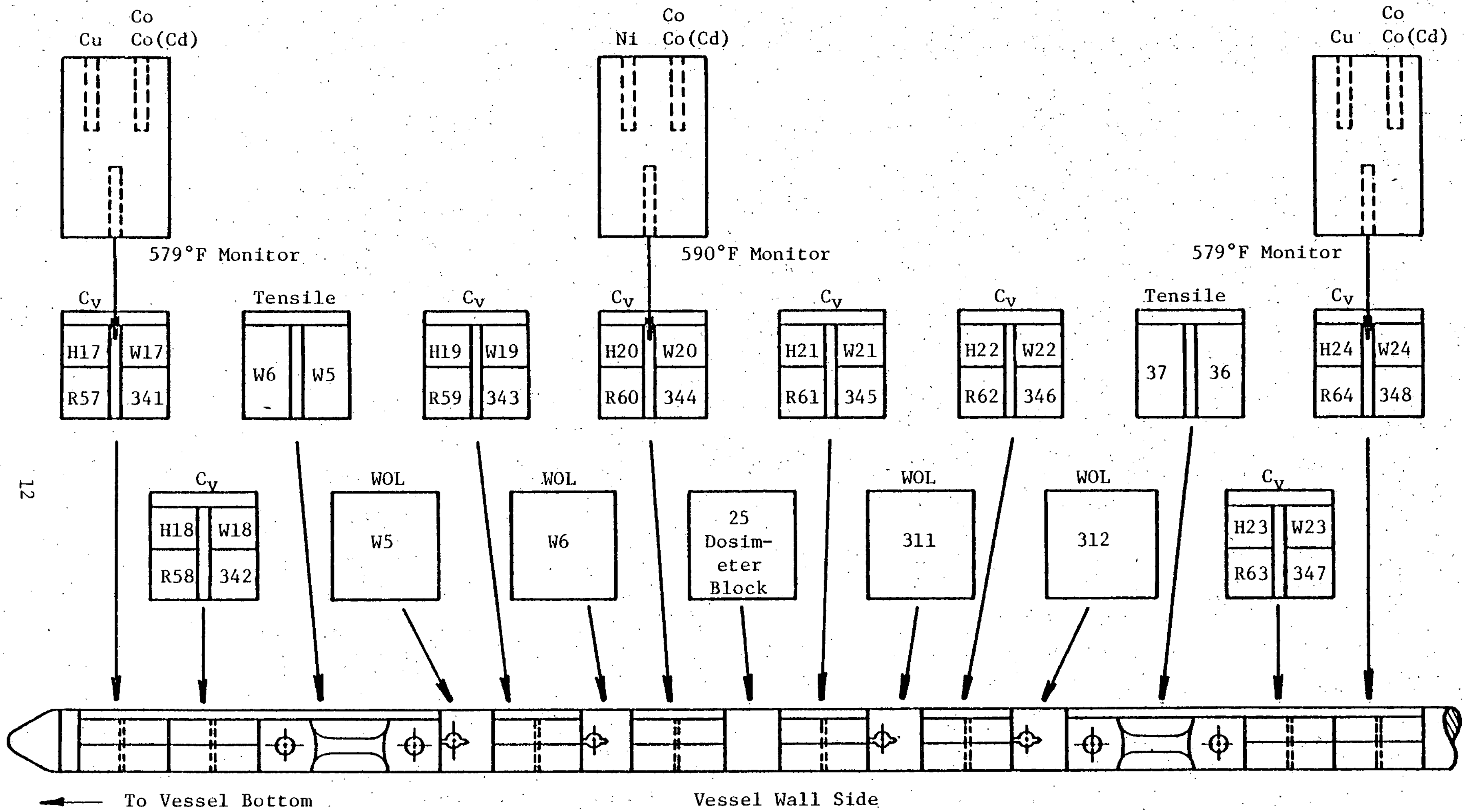

3 = Plate B2002-3   H = HAZ   W = Weld Metal   R = Correlation Monitor Plate

FIGURE 3. ARRANGEMENT OF SPECIMENS AND DOSIMETERS IN CAPSULE Y

IV. TESTING OF SPECIMENS FROM CAPSULE Y

The capsule shipment, capsule opening, specimen testing and reporting of results were carried out in accordance with the following SwRI Nuclear Project Operating Procedures:

(1) XI-MS-1-0, "Determination of Specific Activity of Neutron Radiation Detector Specimen"

(2) XI-MS-3-0, "Conducting Tension Tests on Metallic Materials"

(3) XI-MS-4-0, "Charpy Impact Tests on Metallic Materials"

(4) XIII-MS-1-1, "Opening Radiation Surveillance Capsules and Handling and Storing Specimens"

(5) XI-MS-5-0, "Conducting Wedge-Opening-Loading Tests on Metallic Materials"

(6) XI-MS-6-0, "Determination of Specific Activity of Neutron Radiation Fission Monitor Detector Specimens"

A. Shipment, Opening, and Inspection of Capsule

Southwest Research Institute utilized a procedure which had been prepared for the 1976 refuelling outage for the 1978 removal of Capsule Y from the reactor vessel and the shipment of the capsule to the SwRI laboratories. SwRI contracted with Todd Shipyards - Nuclear Division to supply appropriate cutting tools and a licensed shipping cask. Todd personnel severed the capsule from its extension tube, sectioned the extension tube into three-foot lengths, supervised the loading of the capsule and extension tube materials into the shipping cask, and transported the cask to San Antonio.

The capsule shell had been fabricated by making two long seam welds to join two half-shells together. The long seam welds were milled off on a Bridgeport vertical milling machine set up in one hot cell. Before milling off the long seam weld beads, transverse saw cuts were made to remove the two capsule ends. After the long seam welds had been milled away, the top half of the capsule shell was removed. The specimens and spacer blocks were carefully removed and placed in an indexed receptacle so that capsule location was identifiable. After the disassembly had been completed, the specimens were carefully checked for identification and location, as listed in WCAP 7323.[14]

Each specimen was inspected for identification number, which was checked against the master list in WCAP 7323. No discrepancies were found. The thermal monitors and dosimeter wires were removed from the holes in the spacers. The thermal monitors, contained in quartz vials, were examined and no evidence of melting was observed, thus indicating that the maximum temperature during exposure of Capsule Y did not exceed 579°F.

B. Neutron Dosimetry

The specific activities of the dosimeters were determined at SwRI with an NDC 2200 multichannel analyzer and an NaI(Th) 3 x 3 scintillation crystal. The calibration of the equipment was accomplished with appropriate standards and an interlaboratory cross check with two independent counting laboratories on ^{60}Co-, ^{54}Mn- and ^{58}Co-containing dosimeter wires. All activities were corrected to the time-of-removal (TOR) at reactor shutdown. Infinitely dilute saturated activities (A_{SAT}) were calculated for each of the dosimeters because A_{SAT} is directly related to the product of the energy-dependent microscopic activation cross section and the neutron flux density. The relationship between A_{TOR} and A_{SAT} is given by:

$$\frac{A_{TOR}}{A_{SAT}} = \sum_{m=1}^{m=n} (1-e^{-\lambda T_m})(e^{-\lambda t_m})$$

where: λ = decay constant for the activation product, day^{-1};

T_m = equivalent operating days at 2758 MwTh for operating period m;

t_m = decay time after operating period m, days.

An alternate expression which gives equivalent results is:

$$\frac{A_{TOR}}{A_{SAT}} = \sum_{m=1}^{m=n} P_m(1-e^{-\lambda T_o})(e^{-\lambda t_m})$$

where: T_o = operating days;

P_m = average fraction of full power during operating period.

The Indian Point Unit No. 2 operating history up to the 1978 refuelling shutdown, which was used in the calculation of A_{TOR}, is presented in Table II.

The primary result desired from the dosimeter analysis is the total fast neutron fluence (> 1 MeV) which the surveillance specimens received. The average flux density at full power is given by:

$$\phi = \frac{A_{SAT}}{N_0\bar{\sigma}}$$

where: ϕ = energy-dependent neutron flux density, n/cm^2-sec;

A_{SAT} = saturated activity, dps/mg target element;

$\bar{\sigma}$ = spectrum-averaged activation cross section, cm^2;

N_0 = number of target atoms per mg.

TABLE II

SUMMARY OF REACTOR OPERATIONS
INDIAN POINT UNIT NO. 2

Period (m)	Dates Start	Dates Stop	Shutdown Days	Operating Days, T_m	Decay Time After Period, t_m	Fraction of Full Power in Period, P_m
1	08-15-73	08-24-73	-	10	1634	0.4377
	08-25-73	08-25-73	1	-		
2	08-26-73	09-07-73	-	13	1620	0.4332
	09-08-73	09-20-73	13	-		
3	09-21-73	09-28-73	-	8	1599	0.3161
	09-29-73	09-30-73	2	-		
4	10-01-73	10-12-73	-	12	1585	0.3088
	10-13-73	01-25-74	105	-		
5	01-26-74	01-29-74	-	4	1476	0.2412
	01-30-74	03-21-74	51	-		
6	03-22-74	04-18-74	-	28	1397	0.5438
	04-19-74	04-28-74	10	-		
7	04-29-74	05-03-74	-	5	1382	0.4962
	05-04-74	05-04-74	1	-		
8	05-05-74	05-10-74	-	6	1375	0.4743
	05-11-74	05-12-74	2	-		
9	05-13-74	05-13-74	-	1	1372	0.0730
	05-14-74	05-20-74	7	-		
10	05-21-74	06-14-74	-	25	1340	0.6653
	06-15-74	06-16-74	2	-		
11	06-17-74	07-22-74	-	36	1302	0.7691
	07-23-74	07-23-74	1	-		
12	07-24-74	07-26-74	-	3	1298	0.7593
	07-27-74	08-05-74	10	-		
13	08-06-74	09-06-74	-	32	1256	0.6653
	09-07-74	09-09-74	3	-		
14	09-10-74	09-30-74	-	21	1232	0.7429
	10-01-74	10-11-74	11	-		
15	10-12-74	11-09-74	-	29	1192	0.8637
	11-10-74	11-10-74	1	-		
16	11-11-74	12-06-74	-	26	1165	0.8306
	12-07-74	12-07-74	1	-		
17	12-08-74	01-01-75	-	25	1139	0.8495
	01-02-75	01-04-75	3	-		
18	01-05-75	01-05-75	-	1	1135	0.5430
	01-06-75	01-06-75	1	-		
19	01-07-75	01-31-75	-	25	1109	0.8810
	02-01-75	02-02-75	2	-		
20	02-03-75	02-28-75	-	26	1081	0.9408
	03-01-75	04-03-75	34	-		
21	04-04-75	05-02-75	-	29	1018	0.7652
	05-03-75	05-03-75	1	-		
22	05-04-75	07-28-75	-	86	931	0.9114
	07-29-75	08-10-75	13	-		
23	08-11-75	09-12-75	-	33	885	0.7108
	09-13-75	09-13-75	1	-		
24	09-14-75	10-16-75	-	33	851	0.7962
	10-17-75	10-29-75	13	-		
25	10-30-75	11-14-75	-	16	822	0.7467
	11-15-75	11-15-75	1	-		
26	11-16-75	01-04-76	-	50	771	0.8427
	01-05-76	01-05-76	1	-		
27	01-06-76	01-29-76	-	24	746	0.8703
	01-30-76	02-04-76	6	-		
28	02-05-76	03-30-76	-	55	685	0.9122
	03-31-76	09-26-76	180	-		
29	09-27-76	09-27-76	-	1	504	0.0680
	09-28-76	09-28-76	1	-		
30	09-29-76	10-29-76	-	31	472	0.3423
	10-30-76	12-10-76	42	-		
31	12-11-76	01-27-77	-	48	382	0.8396
	01-28-77	01-29-77	2	-		
32	01-30-77	02-01-77	-	3	377	0.7250
	02-02-77	02-05-77	4	-		
33	02-06-77	03-11-77	-	34	339	0.8825
	03-12-77	03-14-77	3	-		
34	03-15-77	04-10-77	-	27	309	0.9242
	04-11-77	05-13-77	33	-		
35	05-14-77	07-02-77	-	50	226	0.3936
	07-03-77	08-05-77	34	-		
36	08-06-77	08-19-77	-	14	178	0.6372
	08-20-77	08-21-77	2	-		
37	08-22-77	02-13-78	-	176	0	0.9022

Total Power Generation = 853.7 Effective Full Power Days (includes 5.7 EFPD accumulated before 08-15-73).

The total neutron fluence is then equal to the product of the average neutron flux density and the equivalent reactor operating time at full power.

In Capsule Y, the weld metal and HAZ Charpy specimens were located in the specimen layer nearest to the core and the vessel plate and correlation monitor Charpy specimens were located in the specimen layer nearest to the pressure vessel wall. Since there is a radial dependence of the fast neutron flux in the vessel, the neutron exposure received by the weld metal and HAZ Charpy specimens is expected to be higher than that received by the vessel plate and correlation monitor Charpy specimens. The dosimetry program was capable of providing fast neutron flux determinations for each Charpy layer since the copper and nickel threshold detectors were located on the radial centerline of the Charpy specimen layer nearest the core, and the iron threshold detectors were obtained from each layer by cutting the corners off of selected tested Charpy specimens.

Additional dosimetry included the fission monitors located at the radial centerline of the capsule and the thermal neutron monitors (bare and cadmium-shielded cobalt) located at the radial centerline of the Charpy specimen layer nearest the pressure vessel wall.

A discrete ordinates Sn transport analysis for the Indian Point Unit No. 2 reactor vessel was performed by Westinghouse[15] to determine the axial, radial, and azimuthal dependence of the fast neutron ($E > 1.0$ MeV) flux density and energy spectrum within the reactor vessel and surveillance capsules. These results were used to calculate the spectrum-averaged cross-sections for the threshold detectors and the lead factors for use in relating neutron exposure of the pressure vessel to that of the surveillance capsule. The pertinent factors obtained from this transport analysis are summarized in Table III.

The Capsule Y dosimetry results are presented in Table IV. A summary of the fast fluxes calculated for full-power operation follows.

- Fast Flux, Core-Side Charpy Layer. The average value of fast neutron (E > 1 MeV) flux density at the weld metal and HAZ Charpy specimen location was 7.99×10^{10} n/cm^2-sec, based on the results from the iron, copper, and nickel dosimeters. A somewhat lower (7%) result (7.45×10^{10}) would be obtained from the iron dosimeters alone. Using a calculated lead factor of 3.90 (see Table III), the maximum value of neutron flux incident on the pressure vessel wall is predicted to have been 2.05×10^{10} n/cm^2-sec, E > 1 MeV.

- Fast Flux, Vessel-Side Charpy Layer. The average value of fast neutron (E > 1 MeV) flux density at the vessel plate and correlation monitor Charpy specimen location was 6.40×10^{10} n/cm^2-sec, based on the results of the iron dosimetry. Using a calculated lead factor of 3.14 (see Table III), the maximum value of neutron flux incident on the pressure vessel wall is predicted to have been 2.04×10^{10} n/cm^2-sec, E > 1 MeV.

- Fast Flux Capsule Centerline. The results obtained from the fission monitors were completely out of line and it is assumed that there was incomplete recovery of the ^{137}Cs during the chemical separation process.

Averaging the results obtained from the neutron dosimeters located in the two Charpy specimen layers, the peak fast neutron flux incident on the pressure vessel up to the 1978 refueling outage is predicted to have been 2.05×10^{10} n/cm^2-sec, E > 1 MeV, which is 14% higher than the value calculated by Westinghouse, see Table III. The major non-neutronic factors which might contribute to the discrepancy between calculated and measured neutron fluxes include the capsule position in the vessel, the dosimeter positions within the capsule, and the core power distribution.

TABLE III

RESULTS OF DISCRETE ORDINATES Sn TRANSPORT ANALYSIS[15]
INDIAN POINT UNIT NO. 2
CAPSULE Y

A. Calculated Reaction Cross-Sections for Analysis of Fast Neutron Monitors (E > 1.0 MeV)

Reaction	$\bar{\sigma}$ (barns)
$^{54}Fe(n,p)^{54}Mn$	.067
$^{58}Ni(n,p)^{58}Co$	.0899
$^{63}Cu(n,\alpha)^{60}Co$	.000490

B. Calculated Capsule Lead Factors

Position[a]	Location within Capsule	Lead Factor[b]
211.10 cm	Center of core-side Charpy layer	3.90
211.33 cm	Center of capsule	3.72
211.60 cm	Center of two specimen layers	3.52
212.10 cm	Center of vessel-side Charpy layer	3.14

(a) Distance from center of core.

(b) $\frac{\text{Capsule neutron flux density, } E > 1.0 \text{ MeV}}{\text{Maximum neutron flux density at vessel I.D., } E > 1.0 \text{ MeV}}$

C. Calculated Maximum Fast Neutron Flux

Location	Flux, n/cm^2-sec, E > 1.0 MeV
Vessel I.D. Surface	1.78×10^{10}
Vessel Wall 1/4T	1.01×10^{10}
Vessel Wall 3/4T	2.06×10^{9}

D. Calculated Maximum Fast Neutron Fluence for 32 EFPY

Location	Fluence, n/cm^2, E > 1.0 MeV
Vessel I.D. Surface	1.8×10^{19}
Vessel Wall 1/4T	1.0×10^{19}
Vessel Wall 3/4T	2.1×10^{18}

TABLE IV

SUMMARY OF NEUTRON DOSIMETRY RESULTS
INDIAN POINT UNIT NO. 2, CAPSULE Y

Dosimeter Position(a)	Dosimeter Ident.(b)	Activation Reaction	A_{TOR} (dps/mg)	A_{SAT} (dps/mg)	ϕ, E > 1.0 Mev(c) cm^{-2}-sec^{-1}	ϕ, Thermal(c,d) cm^{-2}-sec^{-1}
Core-side	H-24 (Top)	$^{54}Fe(n,p)^{54}Mn$	2.03×10^3	3.33×10^3	7.92×10^{10}	-
	H-22		2.02×10^3	3.31×10^3	7.88×10^{10}	-
	H-20		1.73×10^3	2.84×10^3	6.76×10^{10}	-
	H-19		1.92×10^3	3.14×10^3	7.48×10^{10}	-
	H-17 (Bottom)		1.84×10^3	3.02×10^3	7.19×10^{10}	-
	Cu (Top)	$^{63}Cu(n,\alpha)^{60}Co$	7.64×10^1	3.19×10^2	9.95×10^{10}	-
	Cu (Bottom)		7.37×10^1	3.08×10^2	9.60×10^{10}	-
	Ni (Middle)	$^{58}Ni(n,p)^{58}Co$	3.91×10^4	4.48×10^4	7.16×10^{10}	-
				Avg =	7.99×10^{10}	
Vessel-side	R-64 (Top)	$^{54}Fe(n,p)^{54}Mn$	1.79×10^3	2.93×10^3	6.98×10^{10}	-
	R-62		1.75×10^3	2.88×10^3	6.84×10^{10}	-
	R-60		1.44×10^3	2.37×10^3	5.63×10^{10}	-
	R-59		1.76×10^3	2.88×10^3	6.85×10^{10}	-
	R-57 (Bottom)		1.47×10^3	2.40×10^3	5.72×10^{10}	-
				Avg =	6.40×10^{10}	
Vessel-side	Co (Top)	$^{59}Co(n,\gamma)^{60}Co$	7.37×10^6	3.08×10^7	-	3.84×10^{10}
	CoCd (Top)		3.87×10^6	1.62×10^7		
	Co (Center)		7.95×10^6	3.32×10^7	-	4.50×10^{10}
	CoCd (Center		3.85×10^6	1.61×10^7		
	Co (Bottom)		7.29×10^6	3.05×10^7	-	4.08×10^{10}
	CoCd (Bottom)		3.60×10^6	1.50×10^7		
Centerline	U-238 (Center)	$^{238}U(n,f)^{137}Cs$	1.70×10^3	3.32×10^4	3.9×10^{10}(e)	-
	Np-237 (Center)	$^{237}Np(n,f)^{137}Cs$	2.16×10^3	4.21×10^4	6.0×10^9(e)	-

(a) Core-side Charpy layer, vessel-side Charpy layer, or capsule centerline.
(b) For iron dosimeters, identification refers to Charpy specimens which were sampled.
(c) Calculated flux values subject to a ± 16.5% uncertainty.
(d) Calculated per ASTM Method E 262 using a 37.2 barn 2200 m/sec cross-section.
(e) Probable incomplete recovery of dosimeter material.

Since Indian Point Unit No. 2 operated for 853.7 Effective Full Power Days up to the February 1978 refuelling, the calculated capsule and vessel fluences to that time are as follows:

- Weld Metal and HAZ Charpy Specimens - 5.89×10^{18} n/cm^2
- Vessel Plate and Correlation Monitor Charpy Specimens - 4.72×10^{18} n/cm^2
- Tensile and WOL Specimens - 5.3×10^{18} n/cm^2
- Pressure Vessel ID Surface - 1.5×10^{18} n/cm^2

C. Mechanical Property Tests

The irradiated Charpy V-notch specimens were tested on a SATEC impact machine. The test temperatures were selected to develop the ductile-brittle transition and upper shelf regions. The unirradiated Charpy V-notch impact data reported by Westinghouse(14) and the data obtained by SwRI on the specimens contained in Capsule Y are presented in Tables V through VIII. The Charpy V-notch transition curves for the three plate materials and the correlation monitor material are presented in Figures 4 through 7. The radiation-induced shift in transition temperatures for the vessel plate and HAZ material are indicated at 77 ft-lb and 54 mil lateral expansion as well as at Code-specified levels because the specimens are longitudinally oriented, and this is a method suggested for estimating transverse properties.(16) A summary of the shifts in RT_{NDT} and C_v upper shelf energies for each material are presented in Table IX.

Tensile tests were carried out in the SwRI hot cells using a Dillon 10-000-lb capacity tester equipped with a strain gage extensometer, load cell and autographic recording equipment. Tensile tests were run at room

TABLE V

CHARPY V-NOTCH IMPACT DATA
INDIAN POINT UNIT NO. 2 PRESSURE VESSEL SHELL PLATE B2002-3

Condition	Spec. No.	Temp. (°F)	Energy (ft-lbs)	Shear (%)	Lateral Expansion (mils)
Baseline	(a)	-40	6.5	10	4
		-40	8.0	10	5
		-40	6.0	10	7
		-20	25.5	20	20
		-20	14.0	15	12
		-20	11.0	15	7
		10	41.5	25	33
		10	17.0	25	14
		10	37.5	25	29
		30	34.0	35	30
		30	45.5	35	36
		30	42.5	35	36
		60	54.5	40	45
		60	51.5	40	39
		60	41.0	40	33
		110	71.0	60	60
		110	79.5	70	62
		110	83.5	70	62
		160	116.5	99	83
		160	110.0	95	80
		160	95.5	90	76
		210	109.0	90	80
		210	113.5	100	78
		210	113.0	100	82
Capsule Y	3-41	74	11.0	nil	9
	3-46	160	28.5	10	25
	3-47	210	43.0	20	36
	3-42	235	52.0	40	47
	3-48	260	58.0	50	51
	3-44	300	82.0	100	64
	3-43	350	76.5	100	65
	3-45	400	83.0	100	72

(a) Not reported.

TABLE VI

CHARPY V-NOTCH IMPACT DATA
INDIAN POINT UNIT NO. 2 PRESSURE VESSEL HAZ MATERIAL

Condition	Spec. No.	Temp. (°F)	Energy (ft-lbs)	Shear (%)	Lateral Expansion (mils)
Baseline	(a)	-190	36.5	15	29
		-190	13.0	5	9
		-190	30.5	20	18
		-140	17.0	30	16
		-140	26.0	25	21
		-140	35.5	30	23
		-120	55.5	40	46
		-120	30.0	30	25
		-120	46.0	35	35
		-90	40.0	35	32
		-90	44.0	35	33
		-90	49.5	35	39
		-40	53.0	50	44
		-40	71.5	50	44
		-40	79.0	60	61
		10	90.5	80	72
		10	80.0	75	67
		10	90.0	75	63
		60	103.0	100	83
		60	89.0	95	66
		60	87.5	100	78
		160	112.5	100	80
		160	90.0	100	75
		160	109.0	100	85
Capsule Y	H-21	0	29.5	5	21
	H-17	74	32.0	15	28
	H-20	90	44.5	15	40
	H-19	110	62.5	70	54
	H-23	160	68.5	90	56
	H-24	260	111.5	100	80
	H-18	300	80.0	100	57
	H-22	350	82.0	100	68

(a) Not reported.

TABLE VII

CHARPY V-NOTCH IMPACT DATA
INDIAN POINT UNIT NO. 2 PRESSURE VESSEL WELD METAL

Condition	Spec. No.	Temp. (°F)	Energy (ft-lbs)	Shear (%)	Lateral Expansion (mils)
Baseline	(a)	-150	12.5	10	10
		-150	10.5	15	11
		-100	35.0	25	29
		-100	9.0	20	9
		-100	18.0	30	19
		-80	13.0	20	12
		-80	32.5	20	27
		-80	26.0	20	23
		-40	34.0	30	30
		-40	35.5	35	31
		-40	48.0	35	40
		10	78.5	60	64
		10	74.0	60	60
		10	81.0	70	68
		60	102.5	80	78
		60	102.0	85	82
		60	100.0	85	80
		110	112.5	99	88
		110	108.5	90	87
		110	108.5	98	88
		160	115.5	100	90
		160	113.0	100	92
		160	120.0	100	93
		210	121.0	100	92
		210	123.5	100	91
		210	117.5	100	92
Capsule Y	W-17	74	17.5	nil	14
	W-19	110	23.0	5	19
	W-20	160	40.0	25	34
	W-21	190	47.0	50	43
	W-23	210	55.0	60	53
	W-24	260	71.5	100	51
	W-18[(b)]	300	61.0	100	45
	W-22	350	67.0	100	52

(a) Not reported.
(b) Specimen number stamped on impact side.

TABLE VIII

CHARPY V-NOTCH IMPACT DATA
CORRELATION MONITOR MATERIAL (SUPPLIED BY U. S. STEEL)

Condition	Spec. No.	Temp. (°F)	Energy (ft-lbs)	Shear (%)	Lateral Expansion (mils)
Baseline	(a)	-80	4	2	6
		-80	4	2	6
		-60	8	3	6
		-60	6	3	6
		-40	12	10	14
		-40	10	5	10
		-40	6	5	7
		-20	14	15	14
		-20	13	15	14
		0	22	30	22
		0	18	25	18
		20	29	35	28
		20	23	35	23
		40	36	45	33
		40	26	45	26
		60	36	50	40
		60	33	45	35
		80	67	100	60
		80	50	70	48
		100	68	98	60
		100	62	85	58
Capsule Y	R-60	40	5.0	nil	4
	R-57	74	26.0	5	22
	R-62	90	30.5	10	26
	R-58	110	28.0	15	26
	R-59	135	36.0	20	32
	R-63	160	51.5	40	43
	R-64	210	60.0	90	53
	R-61	260	68.5	100	58

(a) Not reported.

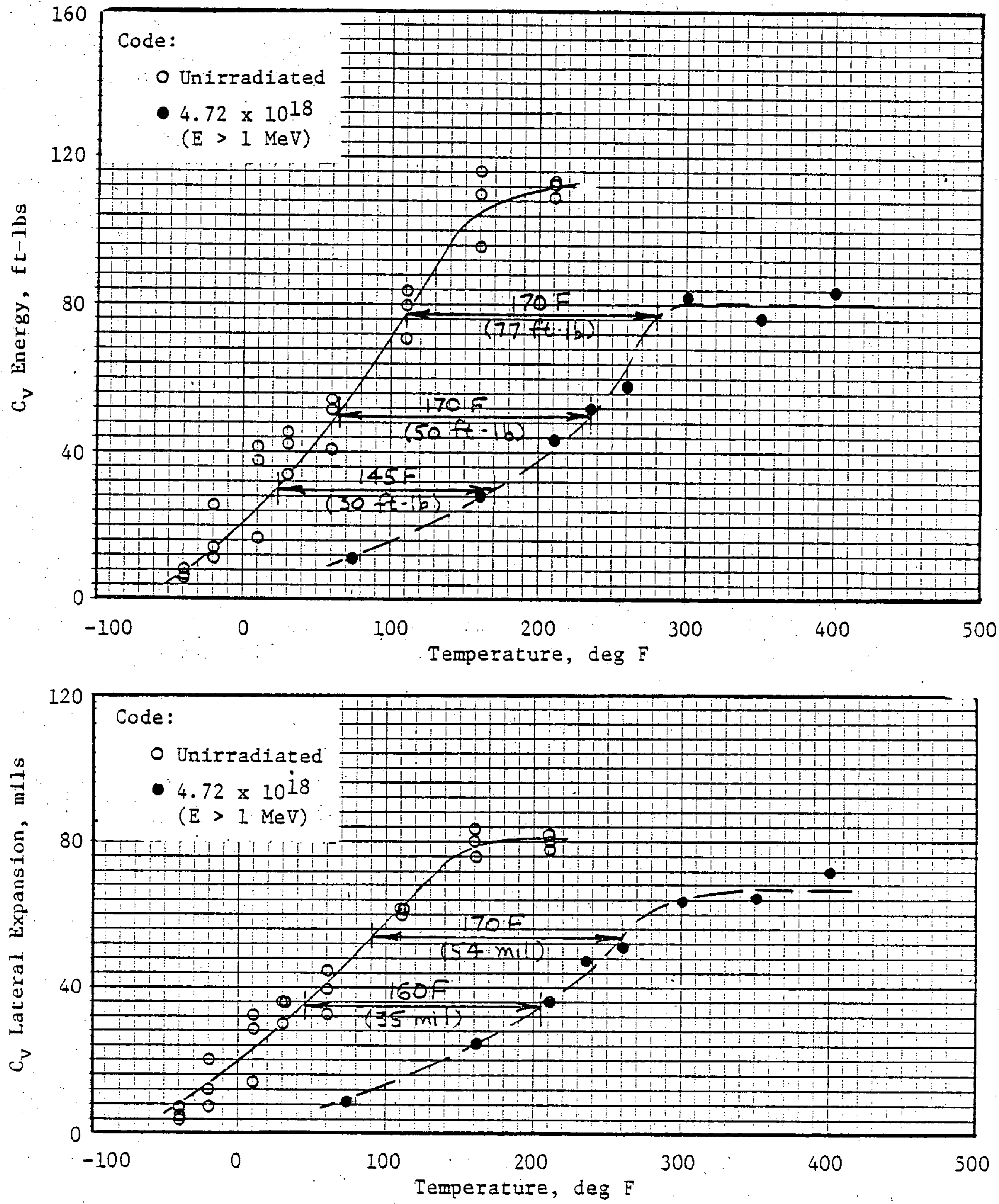

FIGURE 4. EFFECT OF IRRADIATION ON C_v IMPACT PROPERTIES OF INDIAN POINT UNIT NO. 2 SHELL PLATE B2002-3

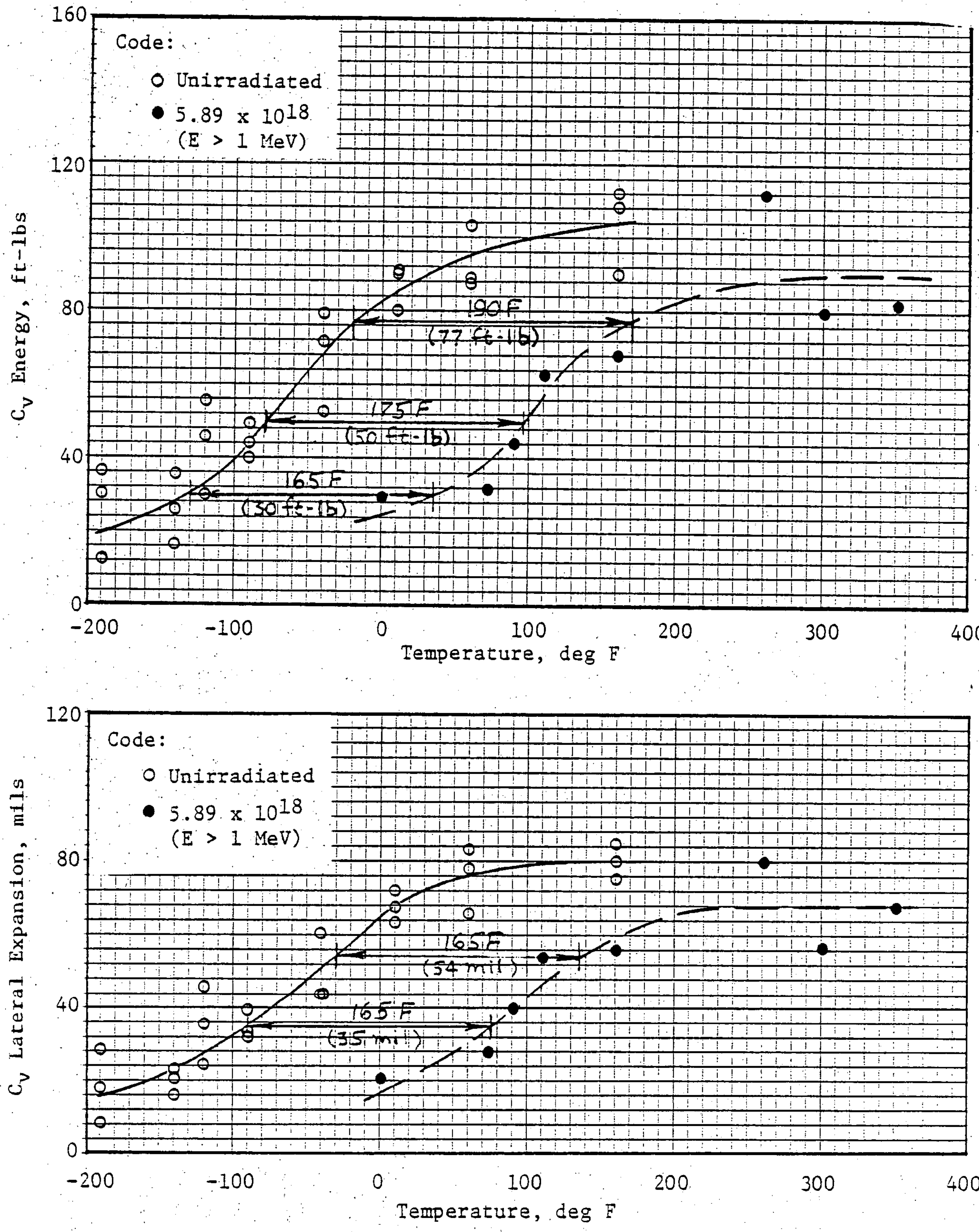

FIGURE 5. EFFECT OF IRRADIATION ON C_V IMPACT PROPERTIES OF INDIAN POINT UNIT NO. 2 HAZ MATERIAL

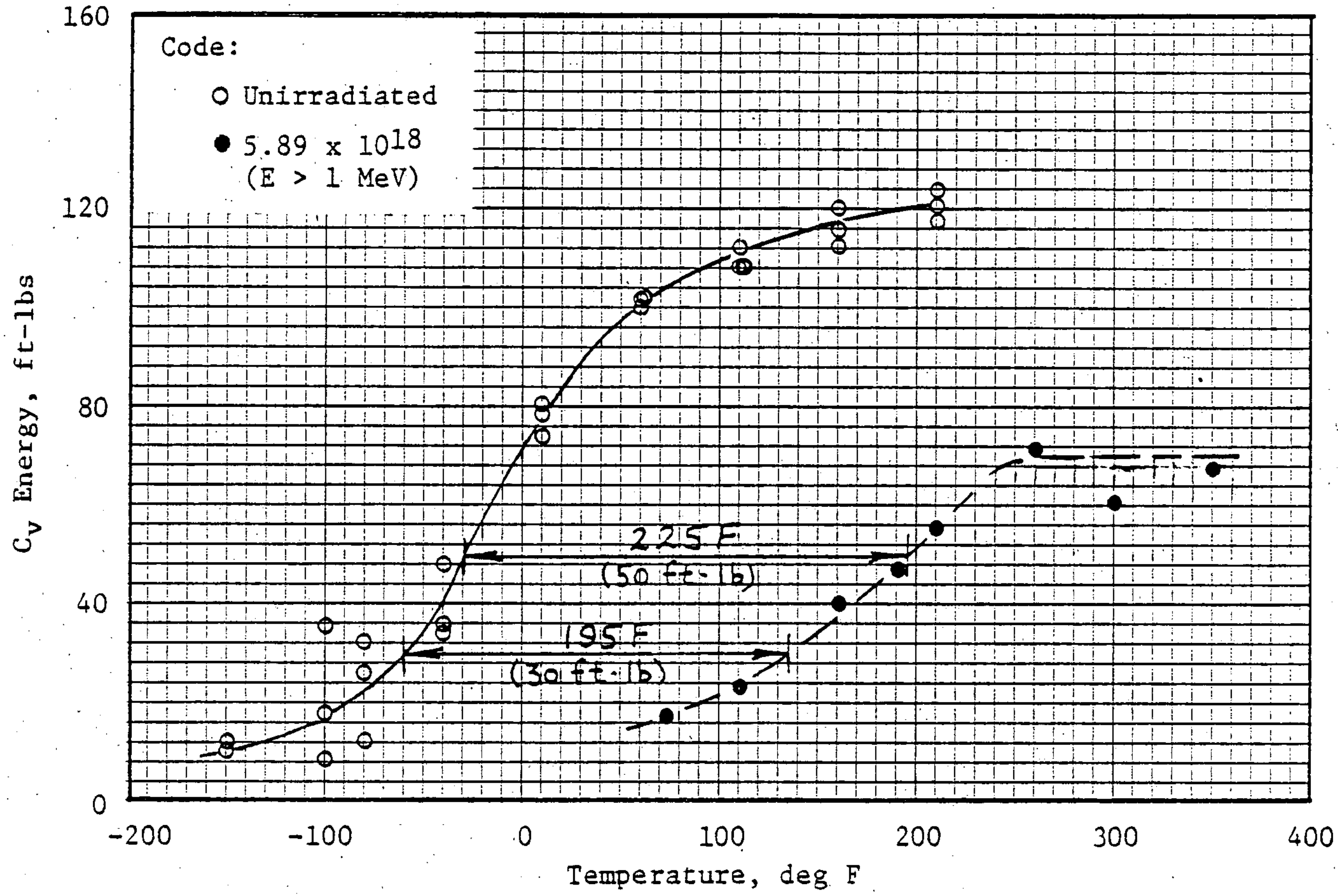

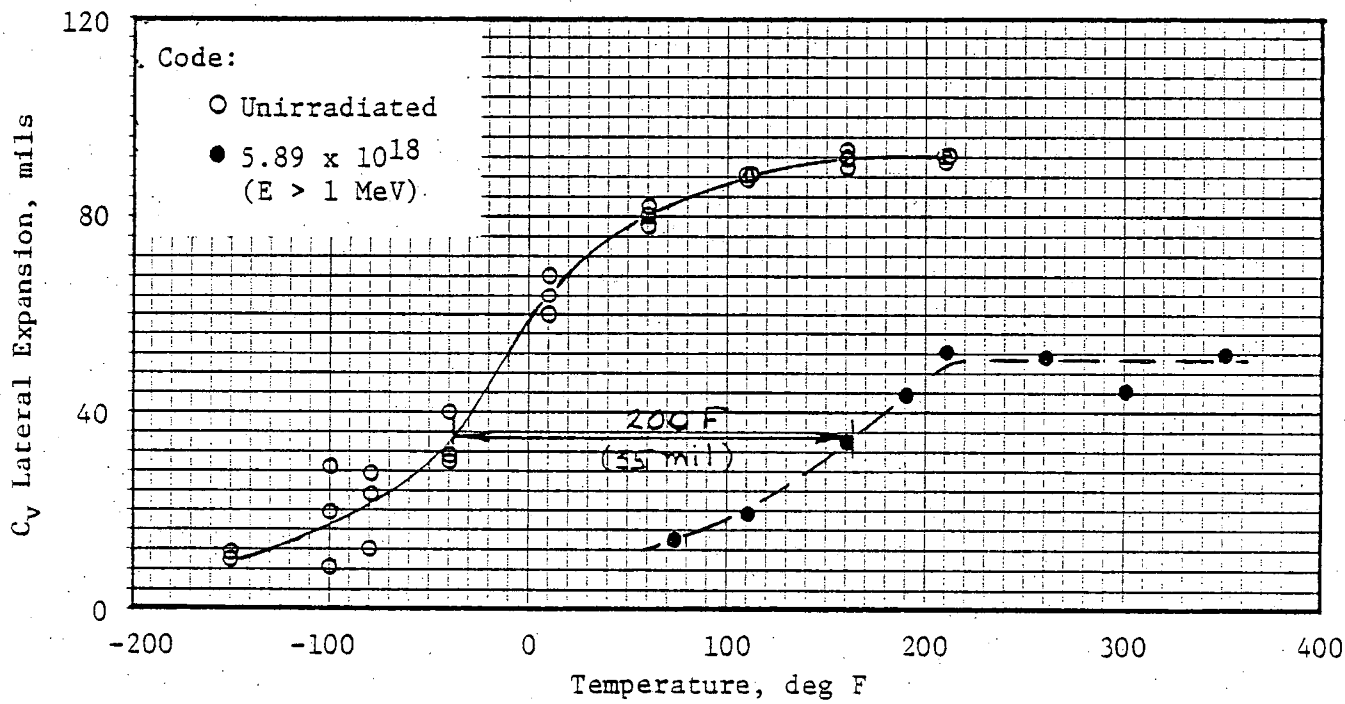

FIGURE 6. EFFECT OF IRRADIATION ON C_v IMPACT PROPERTIES OF INDIAN POINT UNIT NO. 2 WELD METAL

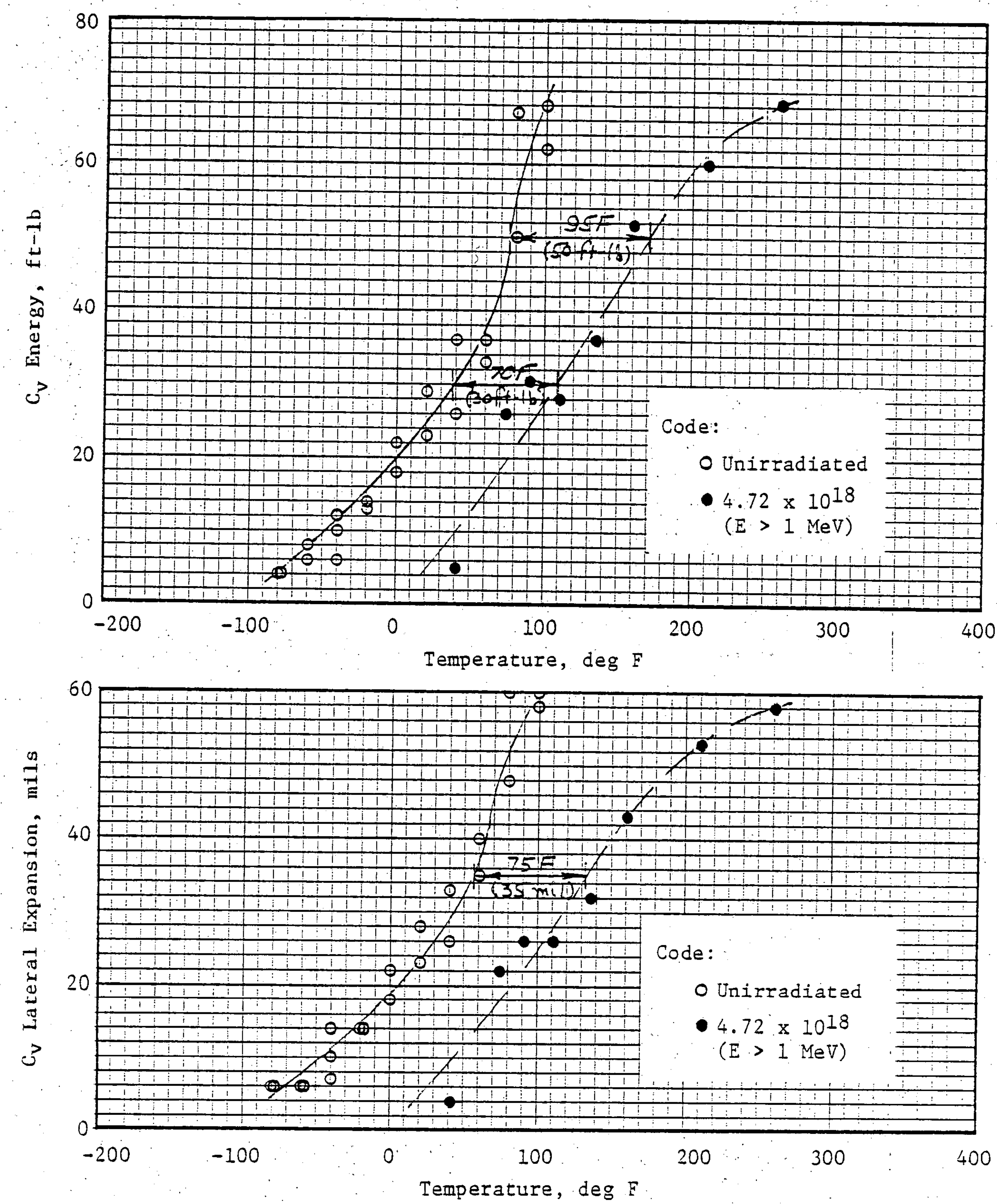

FIGURE 7. EFFECT OF IRRADIATION ON C_V IMPACT PROPERTIES OF INDIAN POINT UNIT NO. 2 CORRELATION MONITOR MATERIAL

TABLE IX

EFFECT OF IRRADIATION ON CAPSULE Y SURVEILLANCE MATERIALS
INDIAN UNIT POINT NO. 2

Criterion(1)	Weld Metal(2)	HAZ Material(2)	Plate B2002-3(3)	Correlation Monitor(3)
Transition Temperature Shift				
@ 77 ft-lb	(4)	190°F	170°F	(4)
@ 50 ft-lb	225°F	175°F	170°F	95°F
@ 30 ft-lb	195°F	165°F	145°F	70°F
@ 54 mil	(4)	165°F	170°F	(4)
@ 35 mil	200°F	165°F	160°F	75°F
ΔRT_{NDT}(5)	225°F	190°F	170°F	95°F
C_V Upper Shelf Drop	49.5 ft-lb (42%)	9 ft-lb (9%)	32.5 ft-lb (29%)	nil

(1) Refer to Figures 4-7.
(2) Fluence = 5.89×10^{18} n/cm^2, E > 1 MeV.
(3) Fluence = 4.72×10^{18} n/cm^2, E > 1 MeV.
(4) Not applicable.
(5) Maximum transition temperature shift by the five criteria.

temperature and 550°F. The results, along with tensile data reported by Westinghouse on the unirradiated materials[14], are presented in Table X. The load-strain records are included in Appendix A.

Testing of the WOL specimens was deferred at the request of Consolidated Edison Company. The specimens are in storage at the SwRI radiation laboratory.

Check analyses for copper and phosphorous content were carried out on eight broken Charpy V-notch specimens, using ASTM Methods E 322[17] and E 350[18], respectively. The following results were obtained:

Material Identification	Specimen No.	% Copper	% Phosphorous
B2002-3	3-41	0.21	.014
B2002-3	3-45	0.22	.012
HAZ Material	H-21	0.15	.014
HAZ Material	H-23	0.20	.020
Weld Metal	W-17	0.19	.010
Weld Metal	W-19	0.22	.017
Correlation Monitor	R-60	0.17	.010
Correlation Monitor	R-62	0.19	.020

The copper contents of the B2002-3 and correlation monitor materials are a little lower than the corresponding results obtained on specimens from Capsule T.[1]

Using the same methods, check analyses for copper and phosphorous on four tested tensile specimens gave the following results:

Material Identification	Specimen No.	% Copper	% Phosphorous
B2002-3	3-6	0.11	.013
B2002-3	3-7	0.10	.012
Weld Metal	W-5	0.18	.022
Weld Metal	W-6	0.20	.025

TABLE X

TENSILE PROPERTIES OF SURVEILLANCE MATERIALS
CAPSULE Y

Condition	Specimen Ident.	Test Temp. (°F)	0.2% Yield Strength (psi)	Tensile Strength (psi)	Total Elongation (%)	Reduction in Area (%)
Baseline	B2002-3	Room	65,650	87,300	27.6	67.3
		Room	65,000	87,350	24.8	66.7
		200	67,800	88,900	23.4	68.6
		200	67,700	89,150	22.1	64.9
		400	57,950	79,550	22.3	68.7
		400	55,350	77,100	23.2	64.9
		600	57,750	83,850	24.9	68.2
		600	58,350	86,500	24.9	64.7
Capsule Y [a]	3-7	Room	76,360	97,780	24.4	65.3
	3-6	550	66,600	90,840	21.2	59.1
Baseline	Weld	Room	64,500	80,700	28.5	73.9
		Room	65,000	81,000	26.9	71.5
		200	63,450	76,100	28.4	72.9
		200	61,050	75,200	25.2	73.0
		400	57,550	75,000	22.9	68.1
		400	58,300	75,800	22.6	69.6
		600	56,650	79,800	24.4	62.0
		600	56,650	79,200	24.0	66.9
Capsule Y [a]	W-6	Room	88,910	102,700	24.7	63.7
	W-5	550	74,330	94,870	20.9	60.2

(a) Fluence = 5.3×10^{18}, E > 1.0 MeV, at radial centerline of test specimens.

The copper contents of the tensile specimens identified as being from plate B2002-3 are in good agreement with previously reported results from Capsule T.[1] It is not known why these results are different from those obtained on the Charpy V-notch specimens.

V. ANALYSIS OF RESULTS

The analysis of data obtained from surveillance program specimens has the following goals:

(1) Estimate the period of time over which the properties of the vessel beltline materials will meet the fracture toughness requirements of Appendix G of 10CFR50. This requires a projection of the measured reduction in C_V upper shelf energy to the vessel wall using knowledge of the energy and spatial distribution of the neutron flux and the dependence of C_V upper shelf energy on the neutron fluence.

(2) Develop heatup and cooldown curves to describe the operational limitations for selected periods of time. This reuqires a projection of the measured shift in RT_{NDT} to the vessel wall using knowledge of the dependence of the shift in RT_{NDT} on the neutron fluence and the energy and spatial distribution of the neutron flux.

The energy and spatial distribution of the neutron flux for Indian Point Unit No. 2 was recently calculated for Capsule Y with a discrete ordinates transport code.[15] This analysis predicted that the lead factor (ratio of fast flux at the capsule location to the maximum pressure vessel flux) for Capsule Y was 3.72 at the capsule centerline, 3.90 for the core-side Charpy layer, and 3.14 for the vessel-side Charpy layer (see Table III). This analysis also predicted that the fast flux at the 1/4T and 3/4T positions in the 8.5-in. pressure vessel wall would be 57% and 12%, respectively, of that at the vessel I.D. However, in this report the projection of Capsule Y results to the pressure vessel wall utilizes the more conservative attenuation figures of 60% and 15% for the 1/4T and

3/4T positions to allow for the increased fraction of neutrons which might accrue in the 0.1 to 1.0 MeV range in deep penetration situations.[19]

A method for estimating the increase in RT_{NDT} as a function of neutron fluence and chemistry is given in Regulatory Guide 1.99, Revision 1.[8] However, the Guide also permits the extrapolation of credible surveillance data by constructing response curves through the data points and parallel to the Guide trend curves, as shown in Figure 8. This plot includes both Capsule T and Capsule Y data.

The Indian Point Unit No. 2 weld metal is more sensitive than the other core beltline materials to irradiation embrittlement. However, because the unirradiated values of RT_{NDT} for the plate materials are much higher than those for the weld metal and HAZ materials[21], the plate material is projected to control the adjusted value of RT_{NDT} through the 32 EFPY design life of Indian Point Unit No. 2. A summary of the projected values of RT_{NDT} for 5, 7, and 32 EFPY of operation is presented in Table XI.

A method for estimating the reduction in C_V upper shelf energy as a function of neutron fluence is also given in Regulatory Guide 1.99, Revision 1.[8] The results from Capsule Y and Capsule T are compared to a portion of Figure 2 of Regulatory Guide 1.99, Revision 1, in Figure 9. The embrittlement response of pressure vessel surveillance materials is in good agreement with the prediction of Regulatory Guide 1.99, Revision 1, except for the low response of the HAZ material.

The projection of the C_V shelf energy of base plate B2002-3 is complicated by the fact that the surveillance specimens are all oriented in the "strong" direction and the 50 ft-lb lower limit of 10CFR50 Appendix G applies to "weak" direction properties. In a method established by the

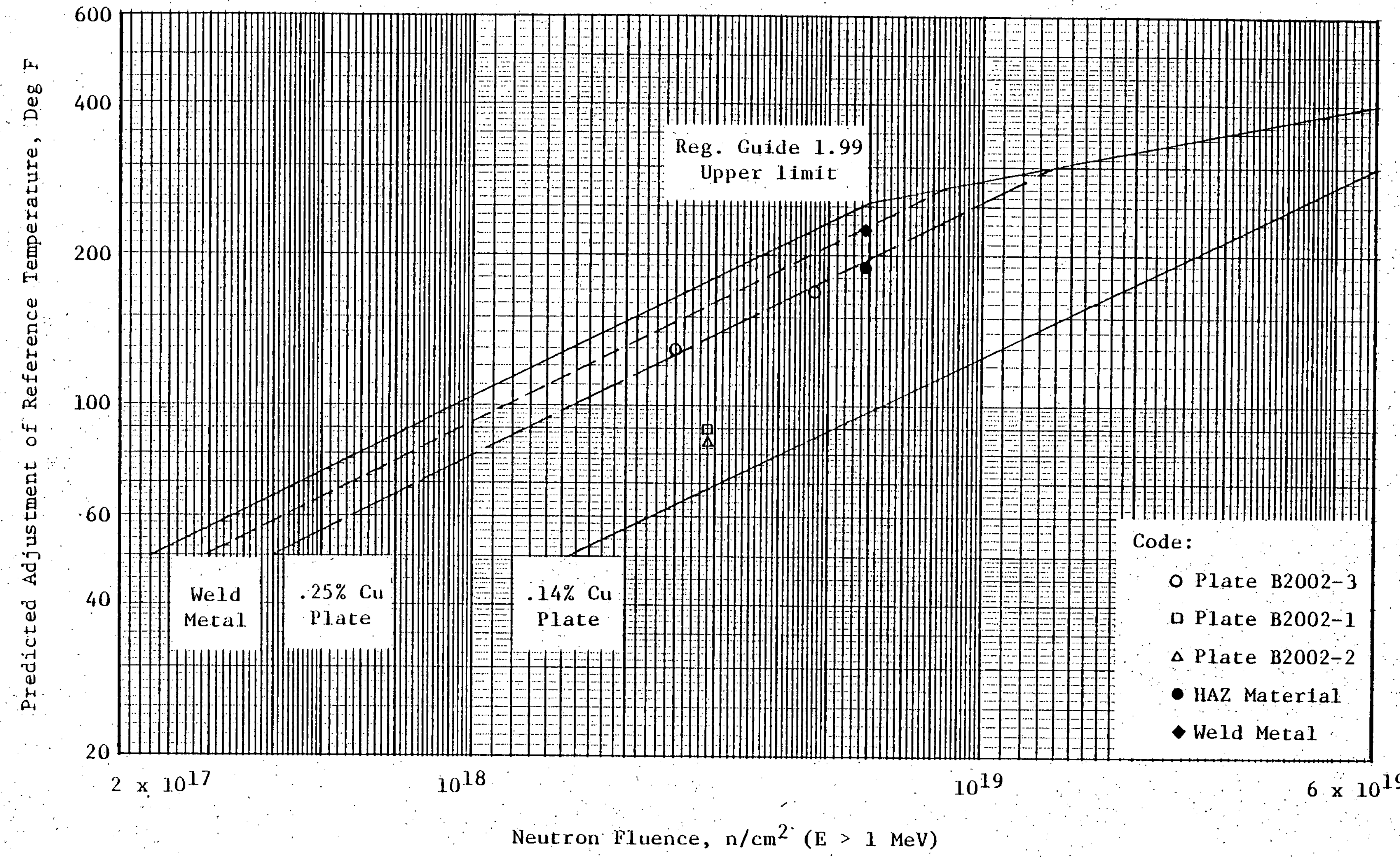

FIGURE 8. EFFECT OF NEUTRON FLUENCE ON RT_{NDT} SHIFT, INDIAN POINT UNIT NO. 2

TABLE XI

ADJUSTED VALUES OF RT_{NDT} FOR INDIAN POINT UNIT NO. 2

EFPY	P.V. Material	Location	Initial RT_{NDT}	Fluence(b)	ΔRT_{NDT}	Adj. RT_{NDT}
5	Plate B2002-3	I.D.	60°F	3.2×10^{18}	145	205
		1/4T	60°F	1.9×10^{18}	110	170
		3/4T	60°F	4.8×10^{17}	55	115
5	HAZ Material	I.D.	-55°F	3.2×10^{18}	145	90
		1/4T	-55°F	1.9×10^{18}	110	55
		3/4T	-55°F	4.8×10^{17}	55	0
5	Weld Metal	I.D.	-45°F	3.2×10^{18}	170	125
		1/4T	-45°F	1.9×10^{18}	130	85
		3/4T	-45°F	4.8×10^{17}	65	20
7	Plate B2002-3	I.D.	60°F	4.5×10^{18}	170	230
		1/4T	60°F	2.7×10^{18}	130	190
		3/4T	60°F	6.8×10^{17}	65	125
7	HAZ Material	I.D.	-55°F	4.5×10^{18}	170	115
		1/4T	-55°F	2.7×10^{18}	130	75
		3/4T	-55°F	6.8×10^{17}	65	10
7	Weld Metal	I.D.	-45°F	4.5×10^{18}	200	155
		1/4T	-45°F	2.7×10^{18}	155	110
		3/4T	-45°F	6.8×10^{17}	75	30
32	Plate B2002-3	I.D.	60°F	2.1×10^{19}	330	390
		1/4T	60°F	1.2×10^{19}	280	340
		3/4T	60°F	3.1×10^{18}	140	200
32	HAZ Material	I.D.	-55°F	2.1×10^{19}	330	275
		1/4T	-55°F	1.2×10^{19}	280	225
		3/4T	-55°F	3.1×10^{18}	140	85
32	Weld Metal	I.D.	-45°F	2.1×10^{19}	330	285
		1/4T	-45°F	1.2×10^{19}	290	245
		3/4T	-45°F	3.1×10^{18}	165	120

(a) 1 EFPY = 1,006,700 MWD_t.
(b) Neutrons/cm^2, E > 1 MeV

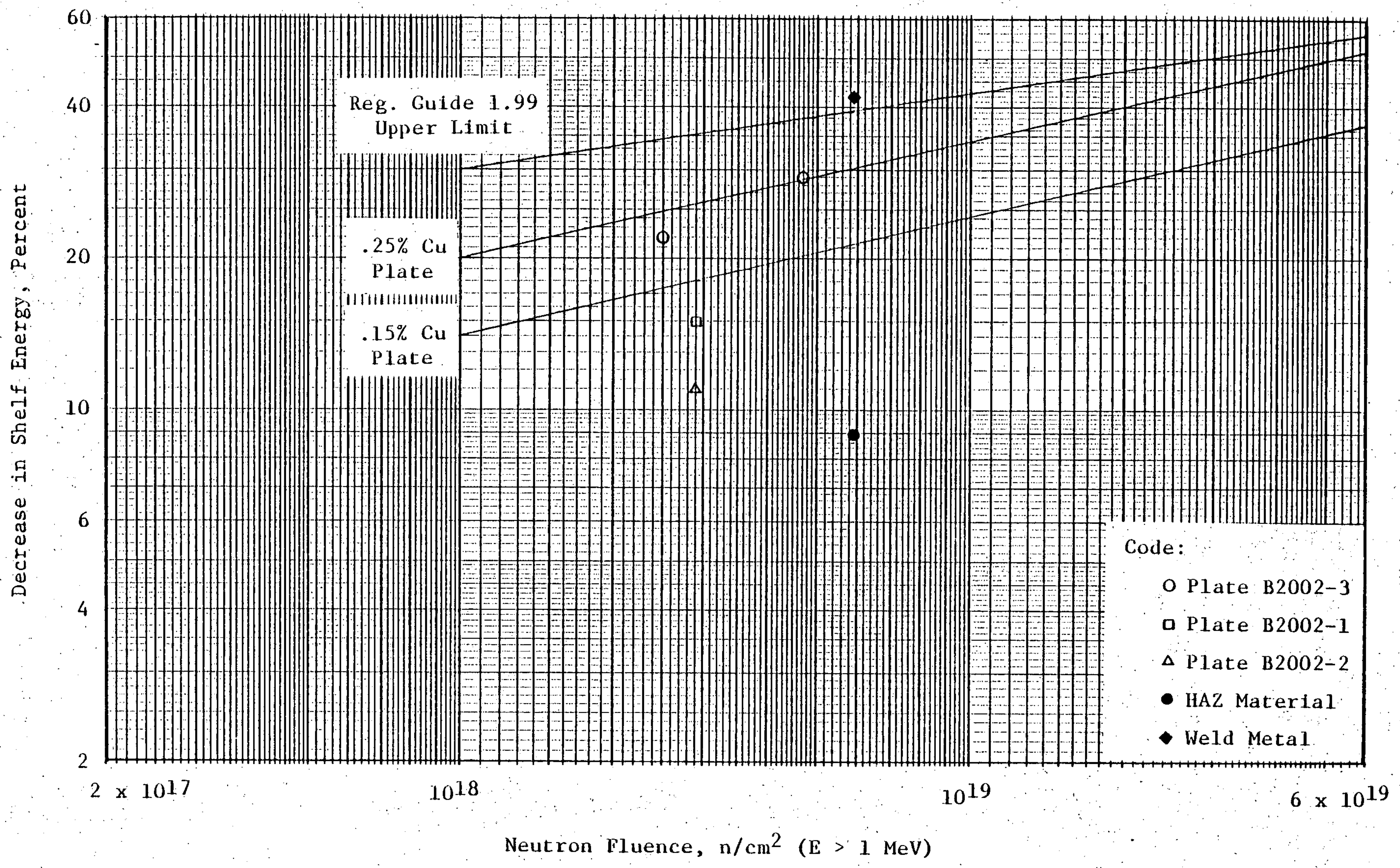

FIGURE 9. DEPENDENCE OF C_V UPPER SHELF ENERGY ON NEUTRON FLUENCE, INDIAN POINT UNIT NO. 2

NRC[20], the estimated upper shelf energy in the "weak" direction is taken to be 65% of that in the "strong" direction. Therefore, the unirradiated C_V shelf energy of plate B2002-3 is estimated to be 73.5 ft-lbs, and this material could sustain a reduction in shelf energy of 32% before reaching 50 ft-lbs. Using the 0.25% Cu (base metal) Regulatory Guide 1.99 curve, it is predicted that the C_V shelf energy of plate B2002-3 will reach 50 ft-lbs at a fluence of about 7.6×10^{18} (E > 1 MeV). This corresponds to approximately 10 EFPY of operation at the vessel I.D. and 17 EFPY at the vessel 1/4T position.

In terms of the normalized shelf energy response, the weld metal is more sensitive than the plate material to irradiation embrittlement. However, the high initial (unirradiated) shelf energy of 118 ft-lb must be reduced by 57.5% to reach 50 ft-lb. Referring to Figure 9, the shelf energy response curve for the weld metal projects that at the vessel I.D., more than 32 EFPY of operation would be required to reduce the shelf energy of the weld metal by this amount. Because of the low sensitivity to radiation embrittlement of the HAZ material, a similar conclusion can be reached concerning its shelf toughness.

The revised Indian Point Unit No. 2 reactor vessel surveillance program, as submitted to NRC[22], is summarized in Table XII. It is consistent with the ASTM National Standard E 185-79 recommendation on removal schedule of surveillance capsules. There are six additional capsules in the vessel, two of which contain weld metal specimens. Capsule Y was removed instead of Capsule S, as originally scheduled, because Capsule Y contained Charpy V-notch specimens from plate B2002-3, the most radiation-sensitive plate material.

TABLE XII

PROPOSED REACTOR VESSEL SURVEILLANCE CAPSULE SCHEDULE
INDIAN POINT UNIT NO. 2

Capsule No.	Capsule Ident.	Capsule Type(a)	Material Content(b)	Scheduled Removal
1	T	I	1,2,3	End of Cycle 1 Operation (Removed 1976)
2	Y	II	3,W,H	End of Cycle 2 Operation (Removed 1978)
3	S	II	1,W,H	End of Cycle 5 Operation
4	Z	I	1,2,3	End of Cycle 8 Operation
5	V	II	2,W,H	End of Cycle 16 Operation
6	U	I	1,2,3	Spare
7	W	I	1,2,3	Spare
8	X	I	1,2,3	Spare

(a) Type I contains all three vessel plates. Type II contains weld metal, HAZ, and one vessel plate.

(b) Material Code: 1 - Plate B2002-1; 2 - Plate B2002-2; 3 - Plate B2002-3; W - Weld Metal; H - HAZ

VI. HEATUP AND COOLDOWN LIMIT CURVES FOR NORMAL OPERATION OF INDIAN POINT UNIT NO. 2

Indian Point Unit No. 2 is a 2758 Mw_t pressurized water reactor operated by Consolidated Edison Company. The unit has been provided with a reactor vessel material surveillance program as required by 10CFR50, Appendix H.

The second surveillance capsule (Capsule Y) was removed during the 1978 refuelling outage. This capsule was tested by Southwest Research Institute, the results being described in the earlier sections of this report. In summary, these results correlate well with those obtained from the first capsule (Capsule T) and indicate that plate B2002-3 will control the value of RT_{NDT} over the plant design lifetime.

The maximum RT_{NDT} after 5 effective full power years (EFPY) of operation was predicted to be 170°F at the 1/4T and 115°F at the 3/4T vessel wall locations, as controlled by plate B2002-3. After 7 EFPY, the corresponding values are predicted to be 190°F and 125°F, respectively. The Unit No. 2 heatup and cooldown limit curves for 5 and 5 to 7 EFPY of operation have been computed on the basis of the above values of RT_{NDT} using procedures described in Appendix B and the following pressure vessel constants:

Vessel Inner Radius, r_i	=	86.50 in.
Vessel Outer Radius, r_o	=	95.28 in.
Operating Pressure, P_o	=	2235 psig
Initial Temperature, T_o	=	70°F
Final Temperature, T_f	=	550°F
Effective Coolant Flow Rate, Q	=	136.3×10^6 lb_m/hr
Effective Flow Area, A	=	26.719 ft^2
Effective Hydraulic Diameter, D	=	15.051 in.

Heatup curves were computed for heatup rates of 60°F/hr and 100°F/hr. Since lower rates tend to raise the curve in the central region (see

Appendix B), the 60°F/hr heatup curve applies to all heating rates up to 60°F/hr. The 100°F/hr heatup curve applies to heatup rates between 60°F/hr and 100°F/hr. Cooldown curves were computed for cooldown rates of 0°F/hr (steady state), 20°F/hr, 60°F/hr, and 100°F/hr. The 20°F/hr curve would apply to cooldown rates up to 20°F/hr; the 60°F/hr curve would apply to rates from 20°F to 60°F/hr; the 100°F/hr curve would apply to rates from 60°F/hr to 100°F/hr.

The Unit No. 2 heatup and cooldown curves for up to 5 EFPY are given in Figures 10, 11, and 12; the heatup and cooldown curves for from 5 to 7 EFPY are given in Figures 13, 14, and 15.

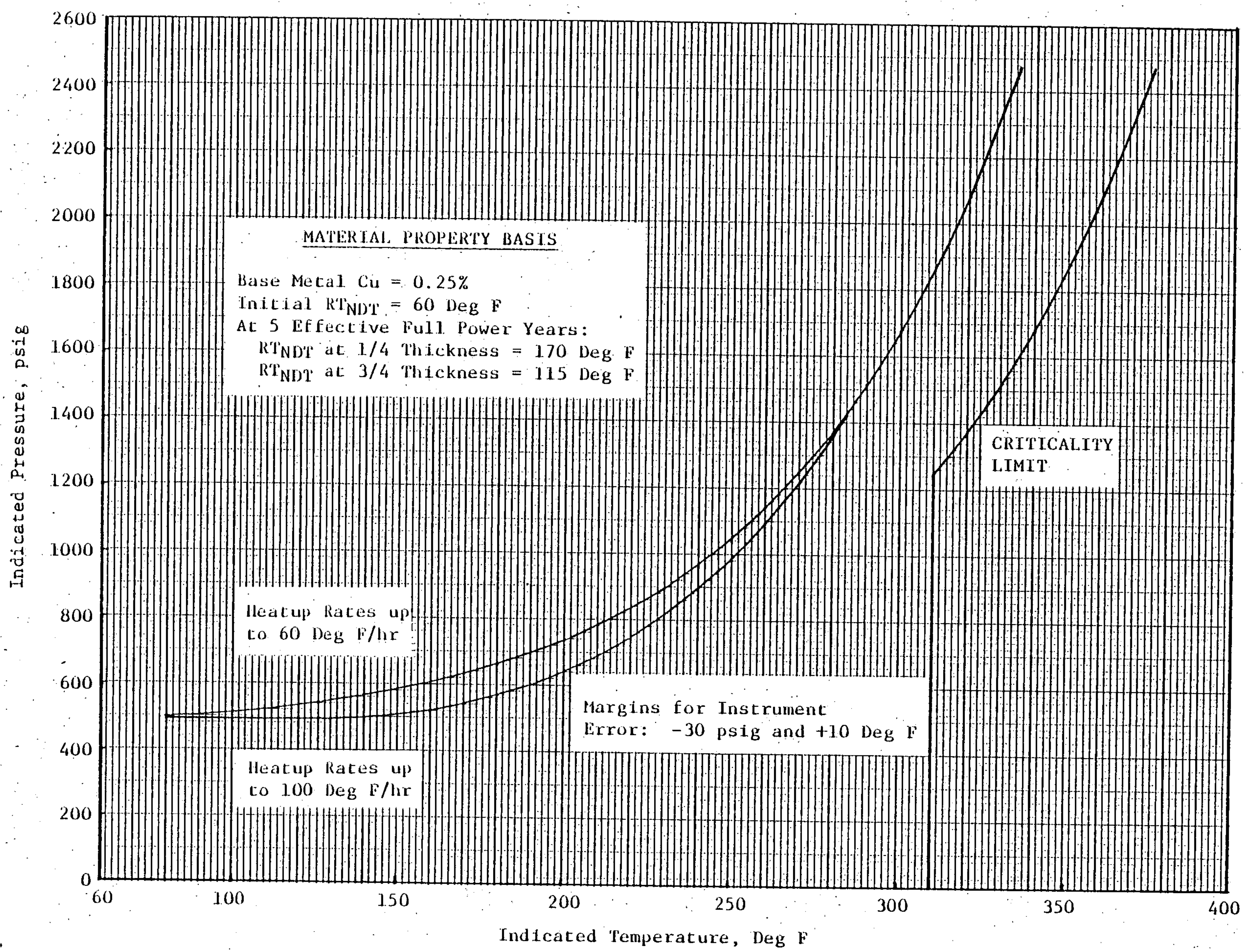

FIGURE 10. INDIAN POINT UNIT NO. 2 REACTOR COOLANT HEATUP LIMITATIONS APPLICABLE FOR PERIODS UP TO 5 EFFECTIVE FULL POWER YEARS

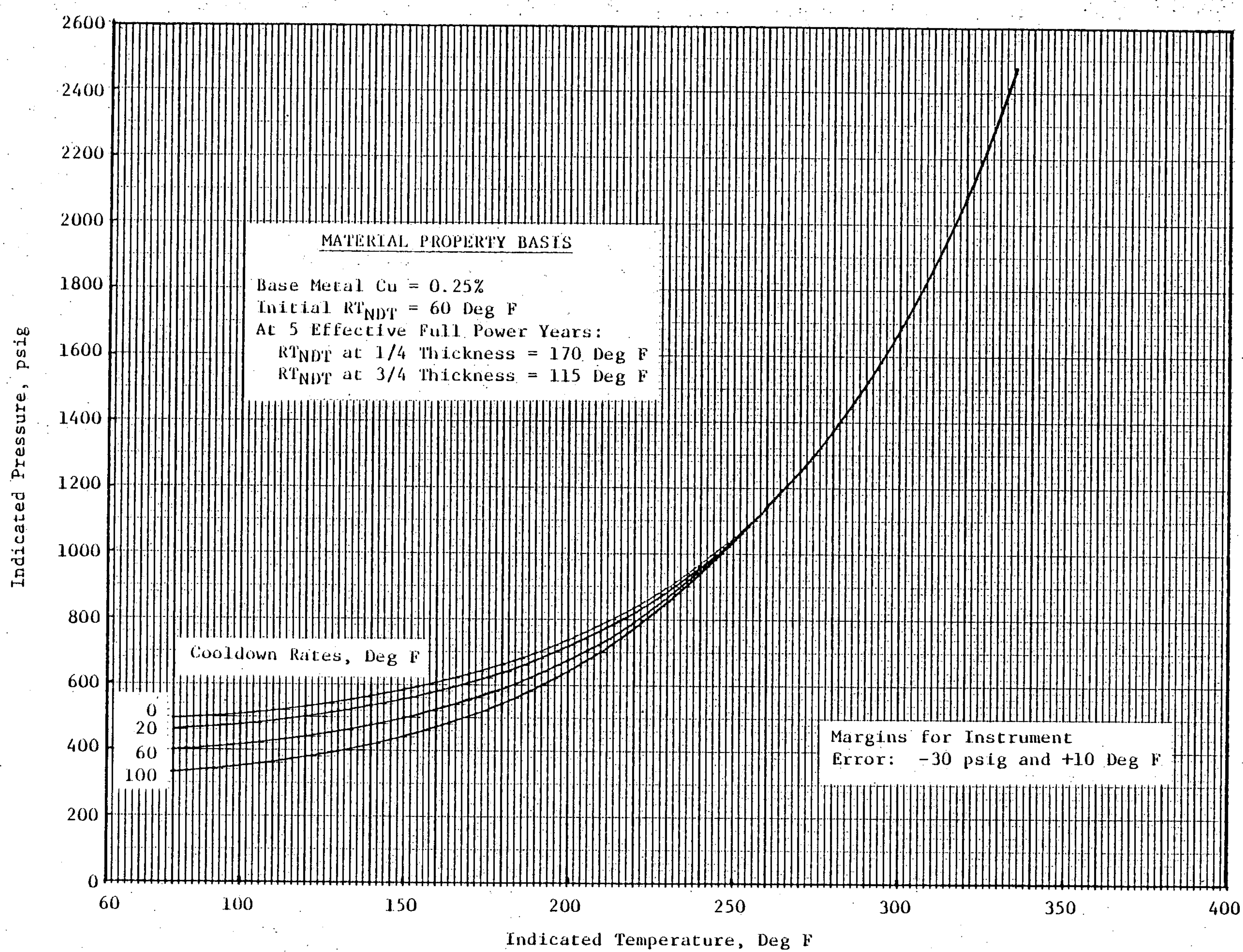

FIGURE 11. INDIAN POINT UNIT NO. 2 COOLANT COOLDOWN LIMITATIONS APPLICABLE FOR PERIODS UP TO 5 EFFECTIVE FULL POWER YEARS

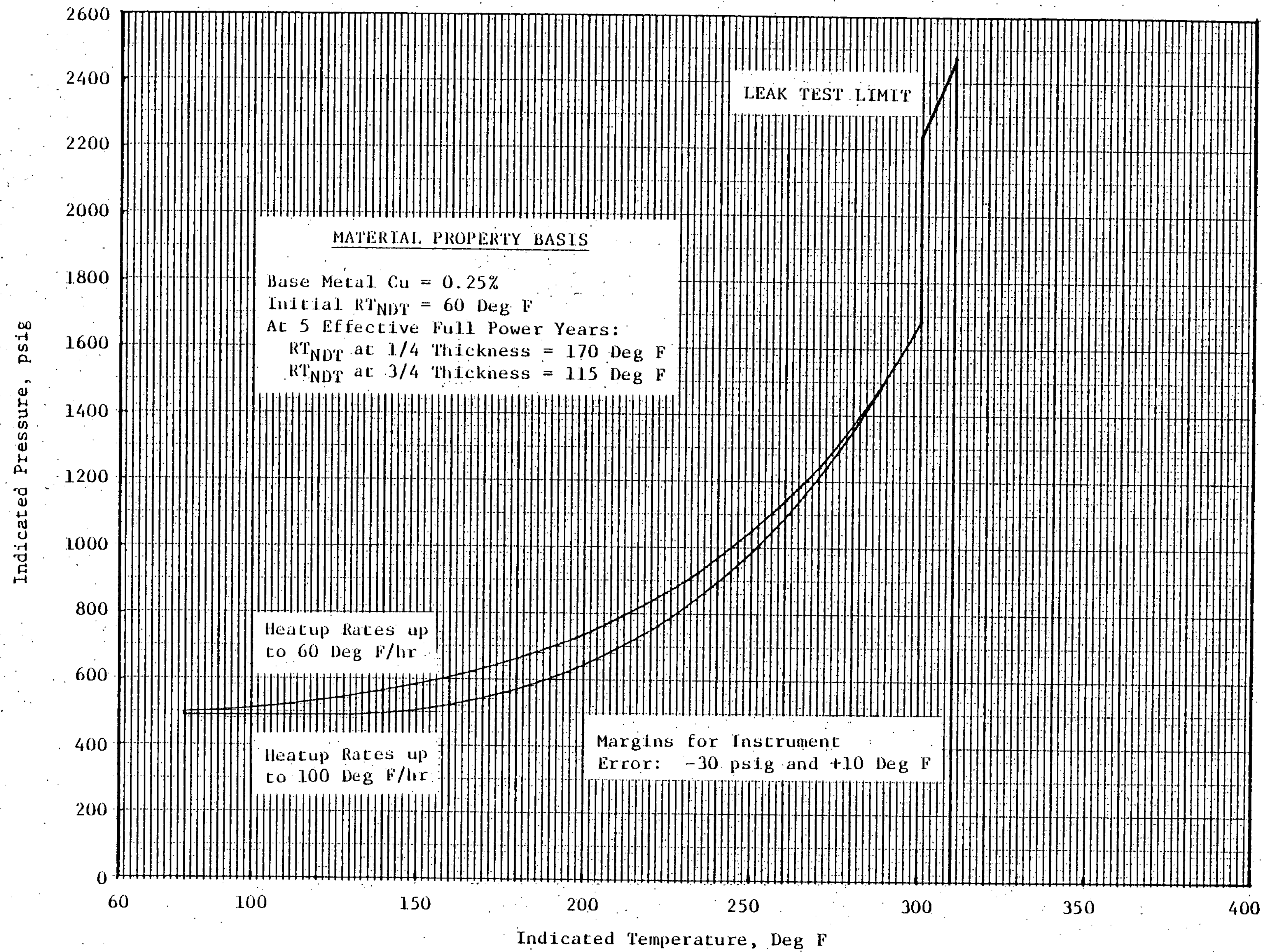

FIGURE 12. INDIAN POINT UNIT NO. 2 LEAK TEST LIMITATIONS APPLICABLE FOR PERIODS UP TO 5 EFFECTIVE FULL POWER YEARS

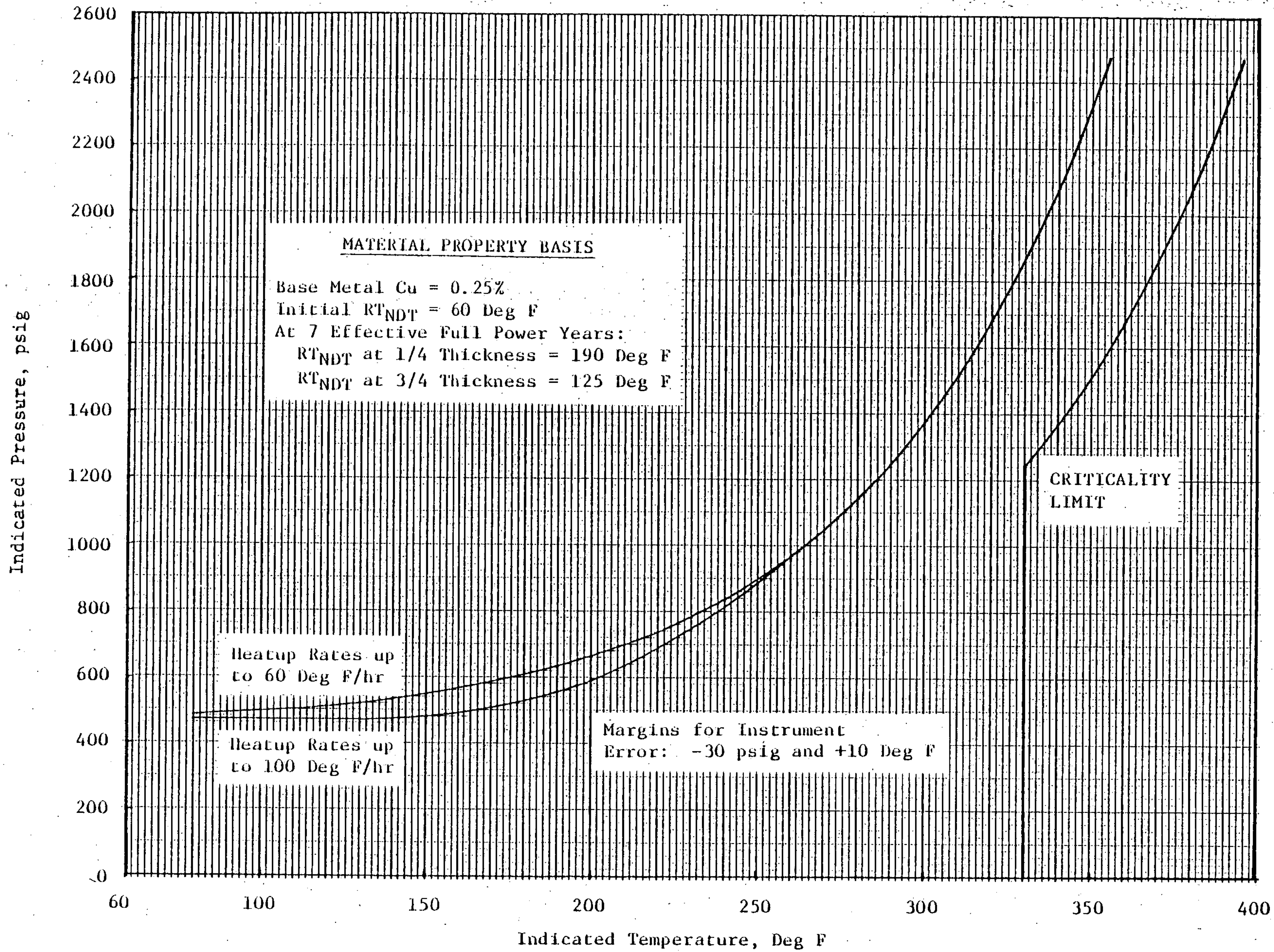

FIGURE 13. INDIAN POINT UNIT NO. 2 REACTOR COOLANT HEATUP LIMITATIONS APPLICABLE FOR THE PERIOD FROM 5 TO 7 EFFECTIVE FULL POWER YEARS

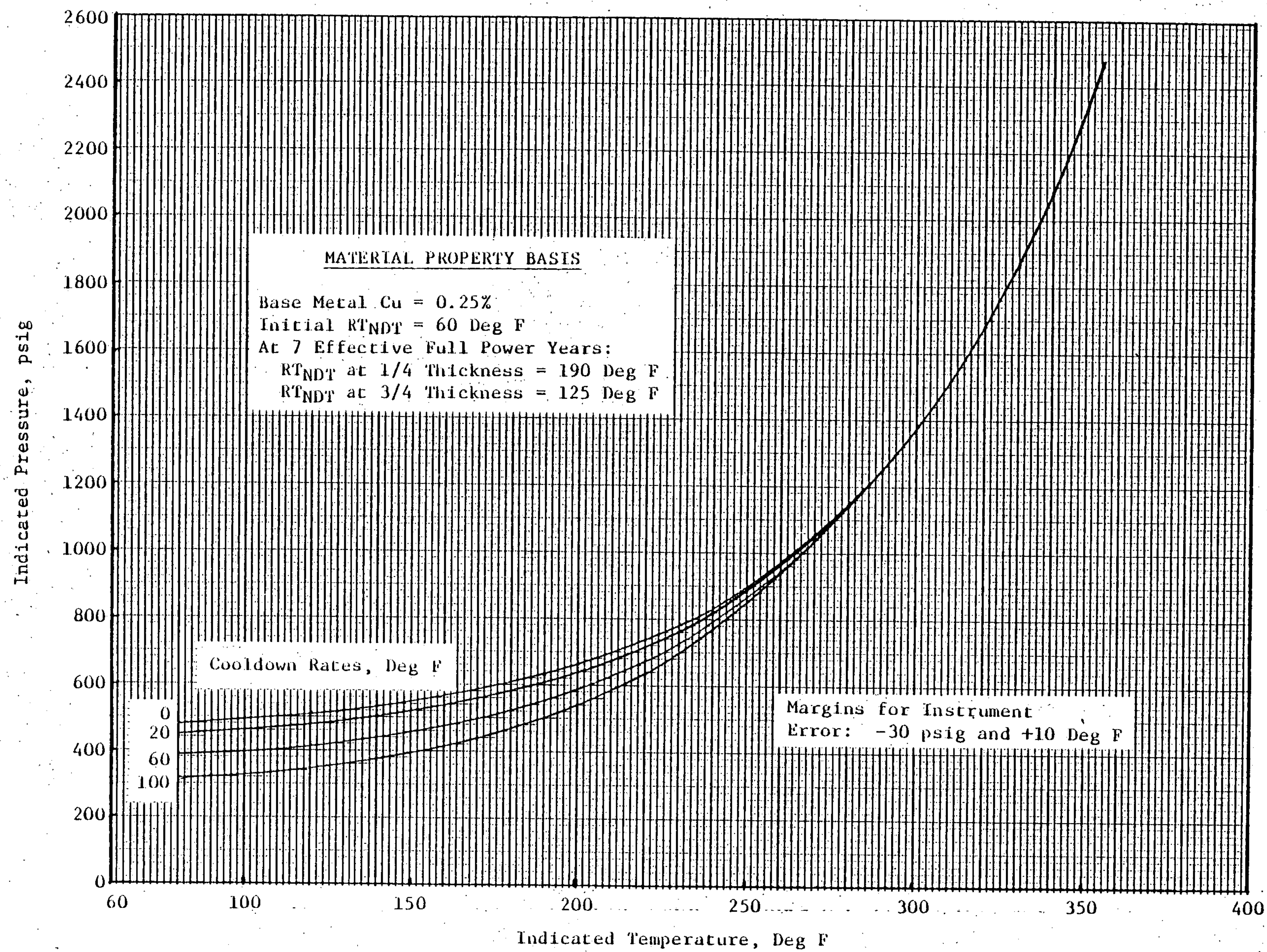

FIGURE 14. INDIAN POINT UNIT NO. 2 REACTOR COOLANT COOLDOWN LIMITATIONS APPLICABLE FOR THE PERIOD FROM 5 TO 7 EFFECTIVE FULL POWER YEARS

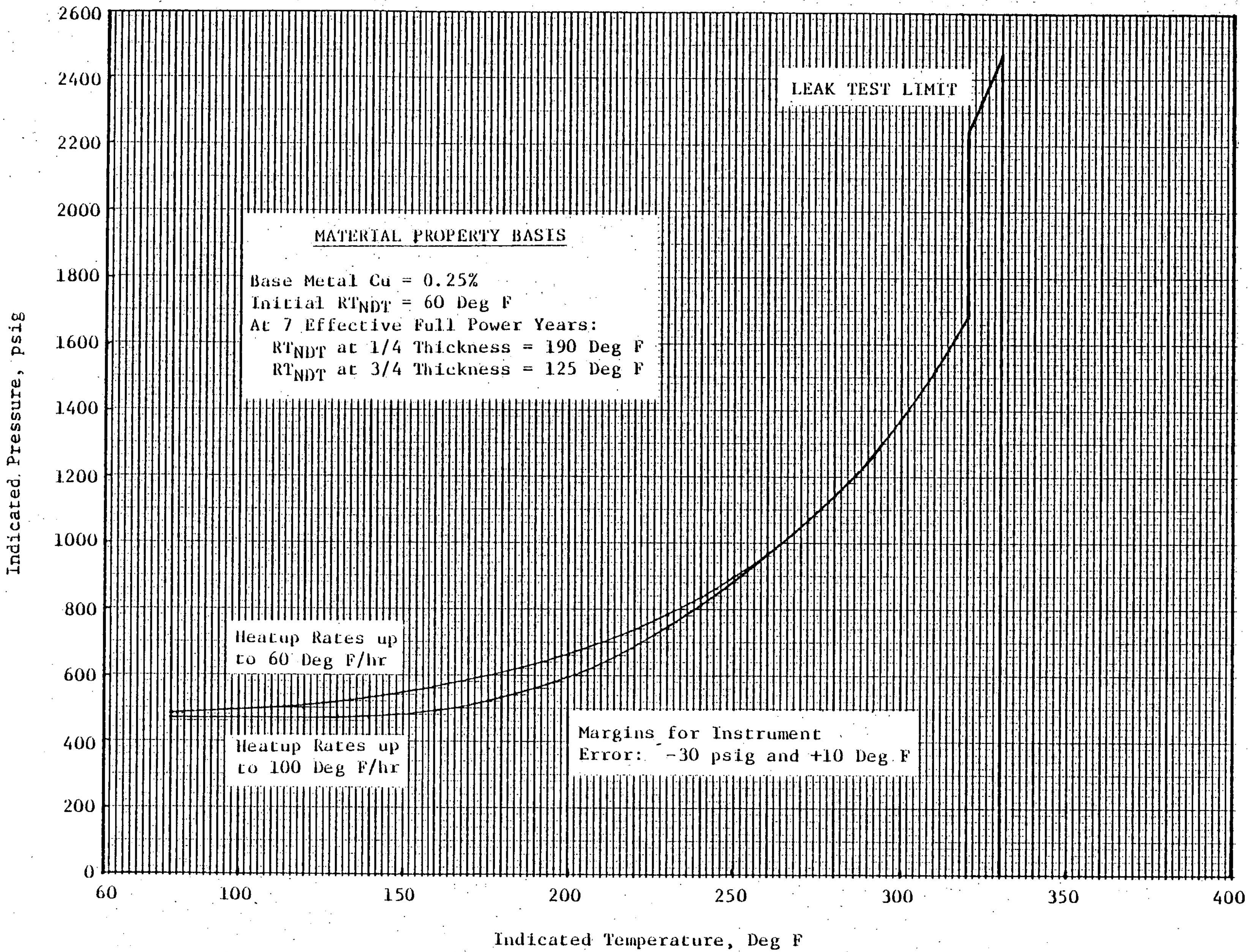

FIGURE 15. INDIAN POINT UNIT NO. 2 LEAK TEST LIMITATIONS APPLICABLE FOR THE PERIOD FROM 5 TO 7 EFFECTIVE FULL POWER YEARS

VII. REFERENCES

1. Norris, E. B., "Reactor Vessel Material Surveillance Program for Indian Point Unit No. 2 -- Analysis of Capsule T," SwRI Report 02-4531, June 30, 1977.

2. Title 10, Code of Federal Regulations, Part 50, "Licensing of Production and Utilization Facilities."

3. ASME Boiler and Pressure Vessel Code, Section III, "Nuclear Power Plant Components," 1974 Edition.

4. ASTM E 208-69, "Standard Method for Conducting Drop-Weight Test to Determine Nil-Ductility Transition Temperature of Ferritic Steels," 1975 Annual Book of ASTM Standards.

5. Steel, L. E., and Serpan, C. Z., Jr., "Analysis of Reactor Vessel Radiation Effects Surveillance Programs," ASTM STP 481, December 1970.

6. Steele, L. E., "Neutron Irradiation Embrittlement of Reactor Pressure Vessel Steels," International Atomic Energy Agency, Technical Reports Series No. 163, 1975.

7. ASME Boiler and Pressure Vessel Code, Section XI, "Rules for Inservice Inspection of Nuclear Power Plant Components," 1974 Edition.

8. Regulatory Guide 1.99, Revision 1, Office of Standards Development, U.S. Nuclear Regulatory Commission, April 1977.

9. Comments on Regulatory Guide 1.99, Westinghouse Electric Corporation, Obtained from NRC Public Document Room, Washington, D.C.

10. Position on Regulatory Guide 1.99, Combustion Engineering Power Systems, Obtained from NRC Public Document Room, Washington, D.C.

11. ASTM E 185-73, "Standard Recommended Practice for Surveillance Tests for Nuclear Reactor Vessels," 1975 Annual Book of ASTM Standards.

12. ASTM E 399-74, "Standard Method of Test for Plane-Strain Fracture Toughness of Metallic Materials," 1975 Annual Book of ASTM Standards.

13. Witt, F. J., and Mager, T. R., "A Procedure for Determining Bounding Values of Fracture Toughness K_{Ic} at Any Temperature," ORNL-TM-3894, October 1972.

14. "Indian Point Unit No. 2 Reactor Vessel Radiation Surveillance Program," WCAP-7323, May 1969.

15. Anderson, S. L., "Analysis of Neutron Flux Levels and Surveillance Capsule Lead Factors for the Indian Point Unit 2 Reactor," July 1979.

16. Hazleton, W. S., Anderson, S. L., and Yanichko, S. E., "Basis for Heatup and Cooldown Limit Curves," WCAP-7924, July 1972.

17. ASTM E 322, "Standard Method for Spectrochemical Analysis of Low Allow Steels and Cast Irons Using an X-ray Fluorescence Spectrometer," 1974 Annual Book of ASTM Standards.

18. ASTM E 350, "Standard Methods for Chemical Analysis of Carbon Steel, Low-Alloy Steel, Silicon Electrical Steel, Ingot Iron, and Wrought Iron," 1978 Annual Book of ASTM Standards.

19. Telecon, E. B. Norris to Ken Hogue (NRC Staff) January 19, 1977.

20. US NRC Standard Review Plan, NUREG-75/087, Section 5.3.2, Pressure-Temperature Limits, November 24, 1975.

21. Indian Point Unit #2 Technical Specifications.

22. Letter, Consolidated Edison Company to Director of Nuclear Reactor Regulation, dated September 24, 1980.

APPENDIX A

TENSILE TEST RECORDS

Southwest Research Institut
Department of Materials Sciences

TENSILE TEST DATA SHEET

Test No. T- 1

Spec. No. W 5

Temperature 550 °F

Strain Rate ______

Est. U.T.S. ______ psi

Initial G. L. 1.000 in.

Initial Dia. .249 in.

Initial Thickness ______ in.

Initial Width ______ in.

Project No. 02-5212-001

Machine No. ______

Date 8/15/78

Initial Area 0.0487

Top Temperature ______ °F

Bottom Temperature ______ °F

Final Gage Length 1.209 in.

Final Diameter .157 in.

Final Area 0.0194 in.^{2}

Maximum Load 4620 lb

0.2% Offset Load 3620 lb

0.02% Offset Load ______ lb

Upper Yield Point ______ lb

$$\text{U.T.S.} = \frac{\text{Maximum Load}}{\text{Initial Area}} = 94{,}870 \text{ psi}$$

$$0.2\% \text{ Y.S.} = \frac{0.2\% \text{ Offset Load}}{\text{Initial Area}} = 74{,}330 \text{ psi}$$

$$0.02\% \text{ Y.S.} = \frac{0.02\% \text{ Offset Load}}{\text{Initial Area}} = \underline{\qquad} \text{ psi}$$

$$\text{Upper Y.S.} = \frac{\text{Upper Yield Point}}{\text{Initial Area}} = \underline{\qquad} \text{ psi}$$

$$\%\ \text{Elongation} = \frac{\text{Final G.L.} - \text{Initial G.L.}}{\text{Initial G.L.}} \times 100 = 20.9\ \%$$

$$\%\ \text{R.A.} = \frac{\text{Initial Area} - \text{Final Area}}{\text{Initial Area}} \times 100 = 60.2\ \%$$

Signature: ______

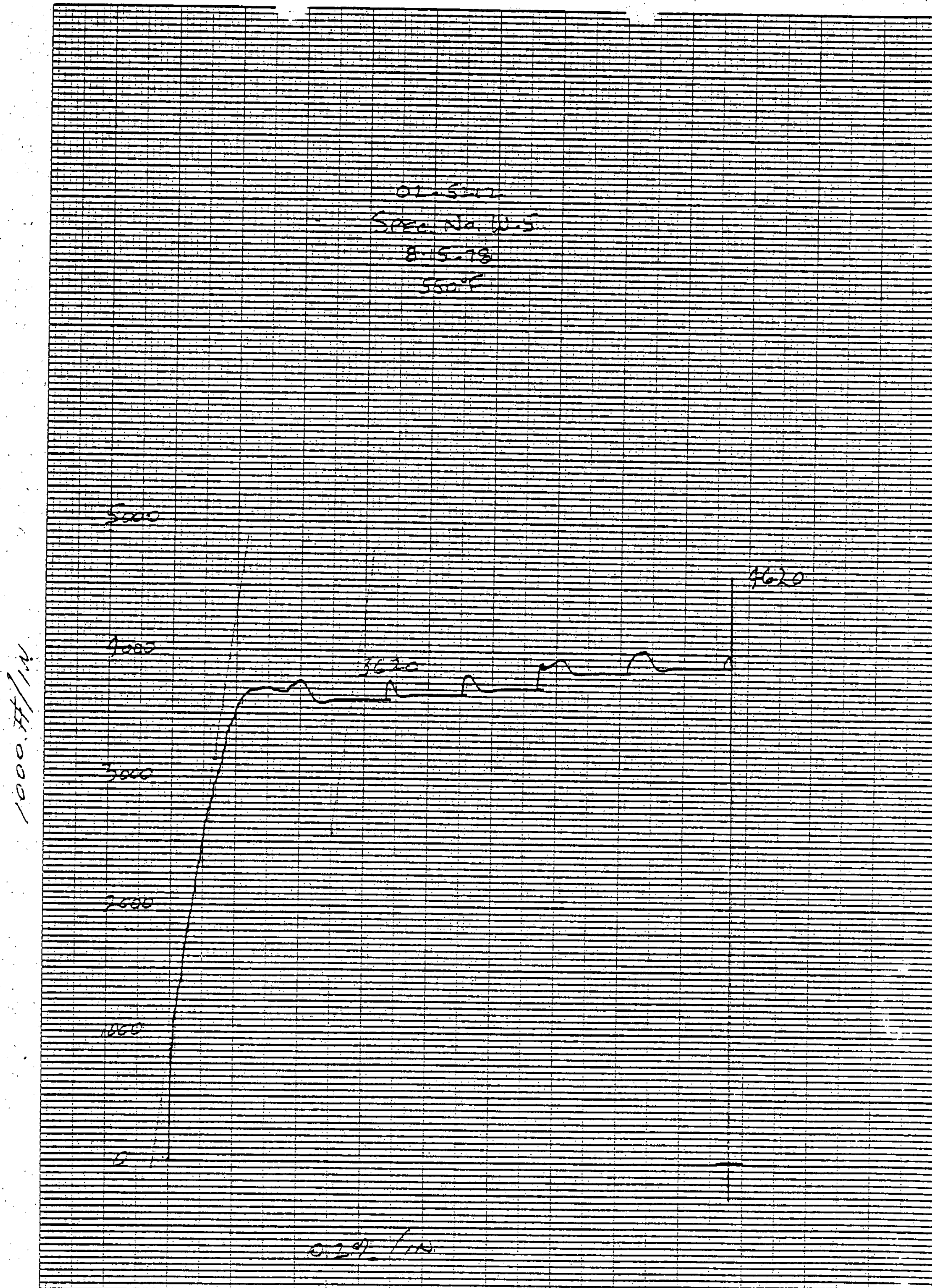

47 1323
K-E 10 X 10 TO ½ INCH • 10 X 15 INCHES
KEUFFEL & ESSER CO. MADE IN U.S.A.

Southwest Research Institute
Department of Materials Sciences

TENSILE TEST DATA SHEET

Test No. T- 2
Spec. No. 3-6
Temperature 550 °F
Strain Rate .01 "/min

Est. U.T.S. ______ psi
Initial G. L. 1.000 in.
Initial Dia. .250 in.
Initial Thickness ______ in.
Initial Width ______ in.

Project No. 02-5212-001
Machine No. DILLON
Date 8-15-78
Initial Area 0.0491

Top Temperature ______ °F
Bottom Temperature ______ °F
Final Gage Length 1.212 in.
Final Diameter .160 in.
Final Area 0.0201 $in.^2$

Maximum Load 4460 lb
0.2% Offset Load 3270 lb
0.02% Offset Load ______ lb
Upper Yield Point ______ lb

$$\text{U.T.S.} = \frac{\text{Maximum Load}}{\text{Initial Area}} = 90,840 \text{ psi}$$

$$0.2\% \text{ Y.S.} = \frac{0.2\% \text{ Offset Load}}{\text{Initial Area}} = 66,600 \text{ psi}$$

$$0.02\% \text{ Y.S.} = \frac{0.02\% \text{ Offset Load}}{\text{Initial Area}} = \_\_\_\_\_\_ \text{ psi}$$

$$\text{Upper Y.S.} = \frac{\text{Upper Yield Point}}{\text{Initial Area}} = \_\_\_\_\_\_ \text{ psi}$$

$$\%\ \text{Elongation} = \frac{\text{Final G. L.} - \text{Initial G. L.}}{\text{Initial G. L.}} \times 100 = 21.2\ \%$$

$$\%\ \text{R. A.} = \frac{\text{Initial Area} - \text{Final Area}}{\text{Initial Area}} \times 100 = 59.1\ \%$$

Signature: ______________________

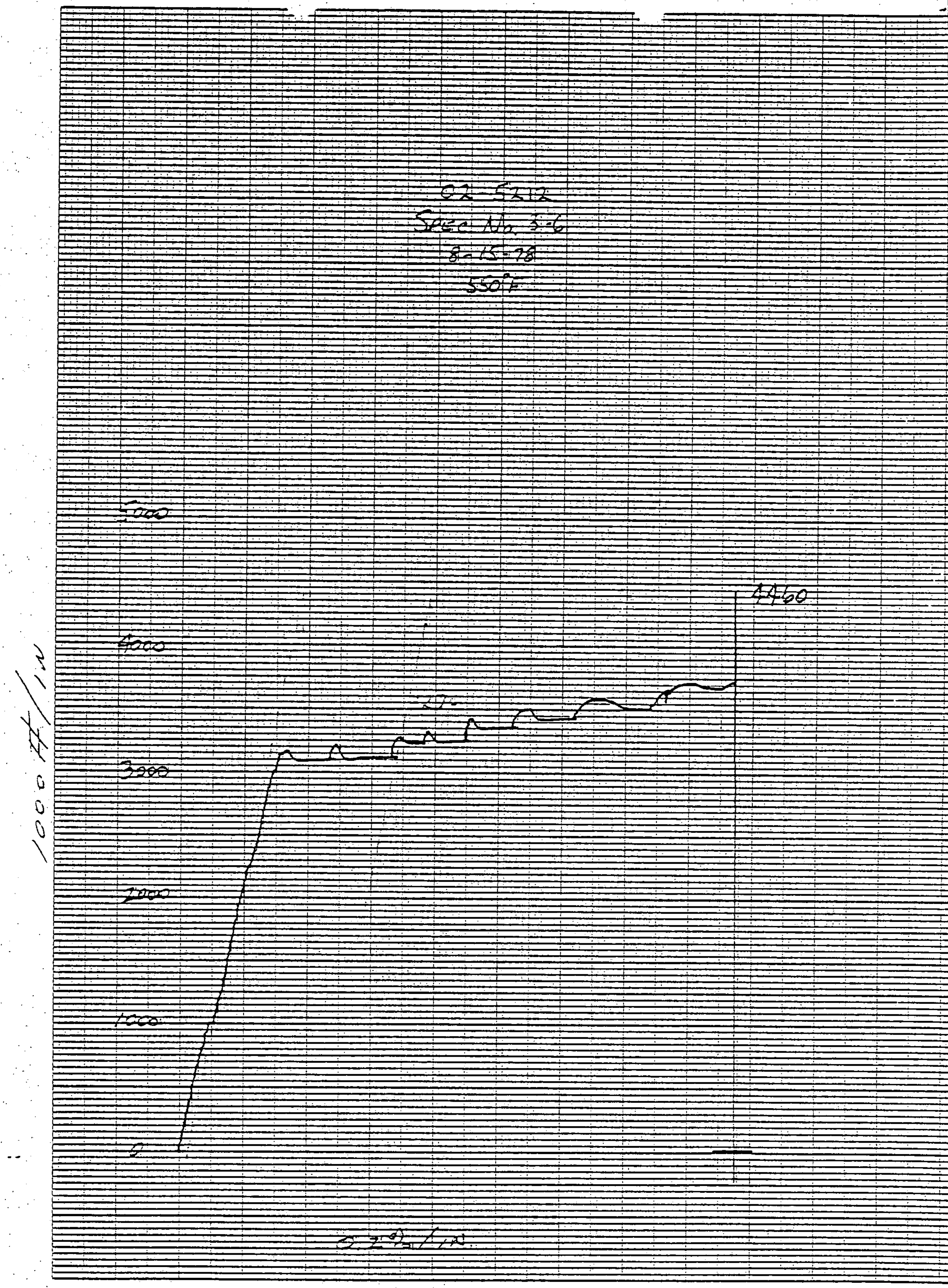

47 1323

K•E 10 X 10 TO ½ INCH • 10 X 15 INCHES
KEUFFEL & ESSER CO. MADE IN U.S.A.

Southwest Research Institute
Department of Materials Sciences

TENSILE TEST DATA SHEET

Test No. T- 3   Est. U.T.S. ______ psi   Project No. 02-5212-001

Spec. No. 3-7   Initial G. L. 1.000 in.   Machine No. DILLON

Temperature 75 °F   Initial Dia. .251 in.   Date 8-23-78

Strain Rate .01 "/MIN   Initial Thickness ______ in.   Initial Area 0.0495

Initial Width ______ in.

Top Temperature ______ °F   Maximum Load 4840 lb

Bottom Temperature ______ °F   0.2% Offset Load 3780 lb

Final Gage Length 1.244 in.   0.02% Offset Load ______ lb

Final Diameter .148 in.   Upper Yield Point ______ lb

Final Area 0.0172 in.^{2}

U.T.S. = $\frac{\text{Maximum Load}}{\text{Initial Area}}$ = 97,780 psi

0.2% Y.S. = $\frac{\text{0.2\% Offset Load}}{\text{Initial Area}}$ = 76,360 psi

0.02% Y.S. = $\frac{\text{0.02\% Offset Load}}{\text{Initial Area}}$ = ______ psi

Upper Y.S. = $\frac{\text{Upper Yield Point}}{\text{Initial Area}}$ = ______ psi

% Elongation = $\frac{\text{Final G. L. - Initial G. L.}}{\text{Initial G. L.}}$ x 100 = 24.4 %

% R. A. = $\frac{\text{Initial Area - Final Area}}{\text{Initial Area}}$ x 100 = 65.3 %

Signature: [signature]

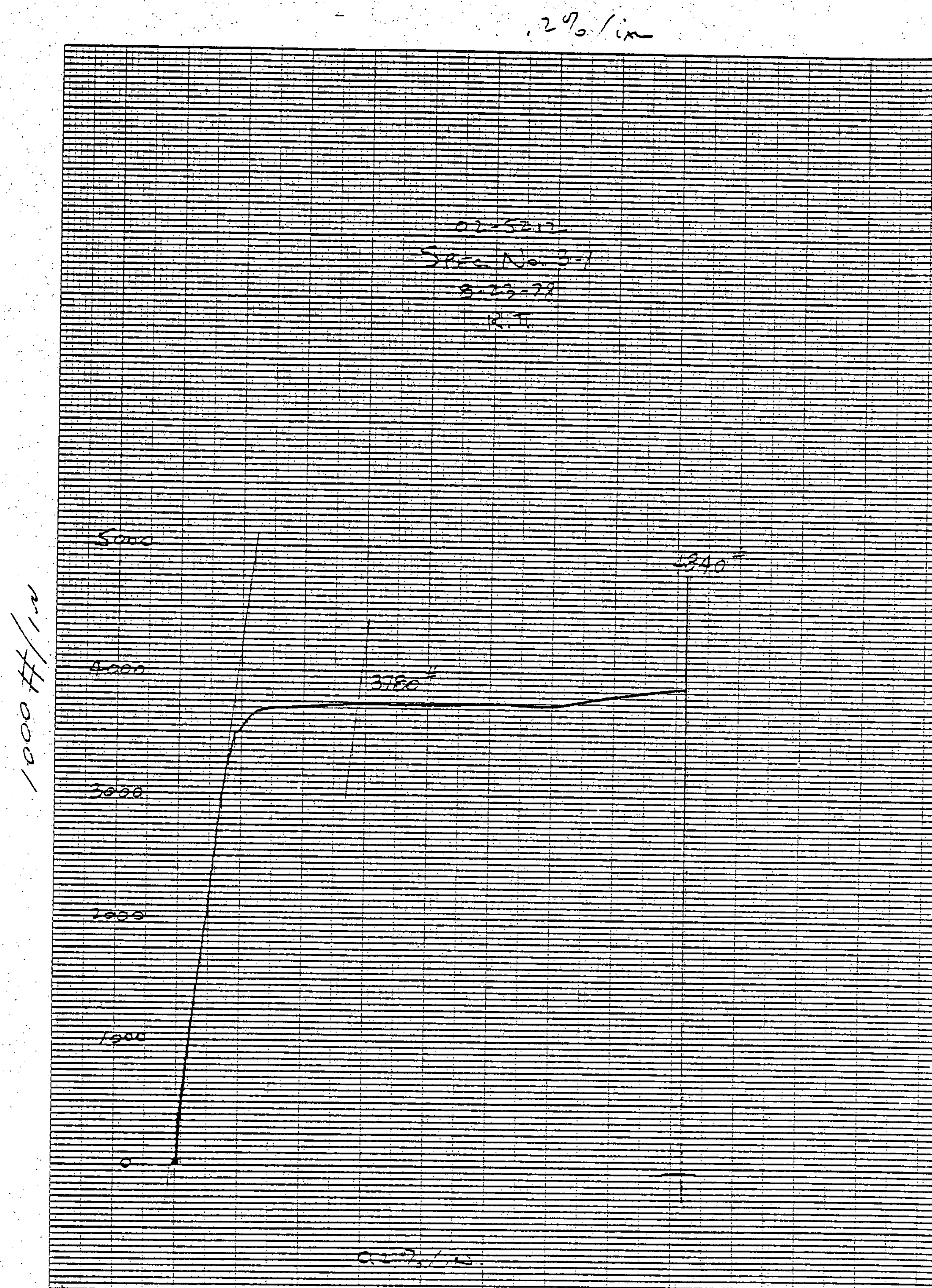

47 1323
K•E 10 X 10 TO ½ INCH • 10 X 15 INCHES
KEUFFEL & ESSER CO. MADE IN U.S.A.

Southwest Research Institute
Department of Materials Sciences

TENSILE TEST DATA SHEET

Test No. T- II4 Est. U.T.S. ______ psi Project No. 02-5212-001

Spec. No. W6 Initial G.L. 1.000 in. Machine No. DILLON

Temperature 75 °F Initial Dia. .249 in. Date 8-23-78

Strain Rate .01"/min Initial Thickness ______ in. Initial Area 0.0487

Initial Width ______ in.

Top Temperature ______ °F Maximum Load 5000 lb

Bottom Temperature ______ °F 0.2% Offset Load 4330 lb

Final Gage Length 1.247 in. 0.02% Offset Load ______ lb

Final Diameter .150 in. Upper Yield Point ______ lb

Final Area 0.0177 in.^{2}

U.T.S. = $\frac{\text{Maximum Load}}{\text{Initial Area}}$ = 102,700 psi

0.2% Y.S. = $\frac{\text{0.2\% Offset Load}}{\text{Initial Area}}$ = 88,910 psi

0.02% Y.S. = $\frac{\text{0.02\% Offset Load}}{\text{Initial Area}}$ = ______ psi

Upper Y.S. = $\frac{\text{Upper Yield Point}}{\text{Initial Area}}$ = ______ psi

% Elongation = $\frac{\text{Final G.L. - Initial G.L.}}{\text{Initial G.L.}}$ x 100 = 24.7 %

% R.A. = $\frac{\text{Initial Area - Final Area}}{\text{Initial Area}}$ x 100 = 63.7 %

Signature: [signature]

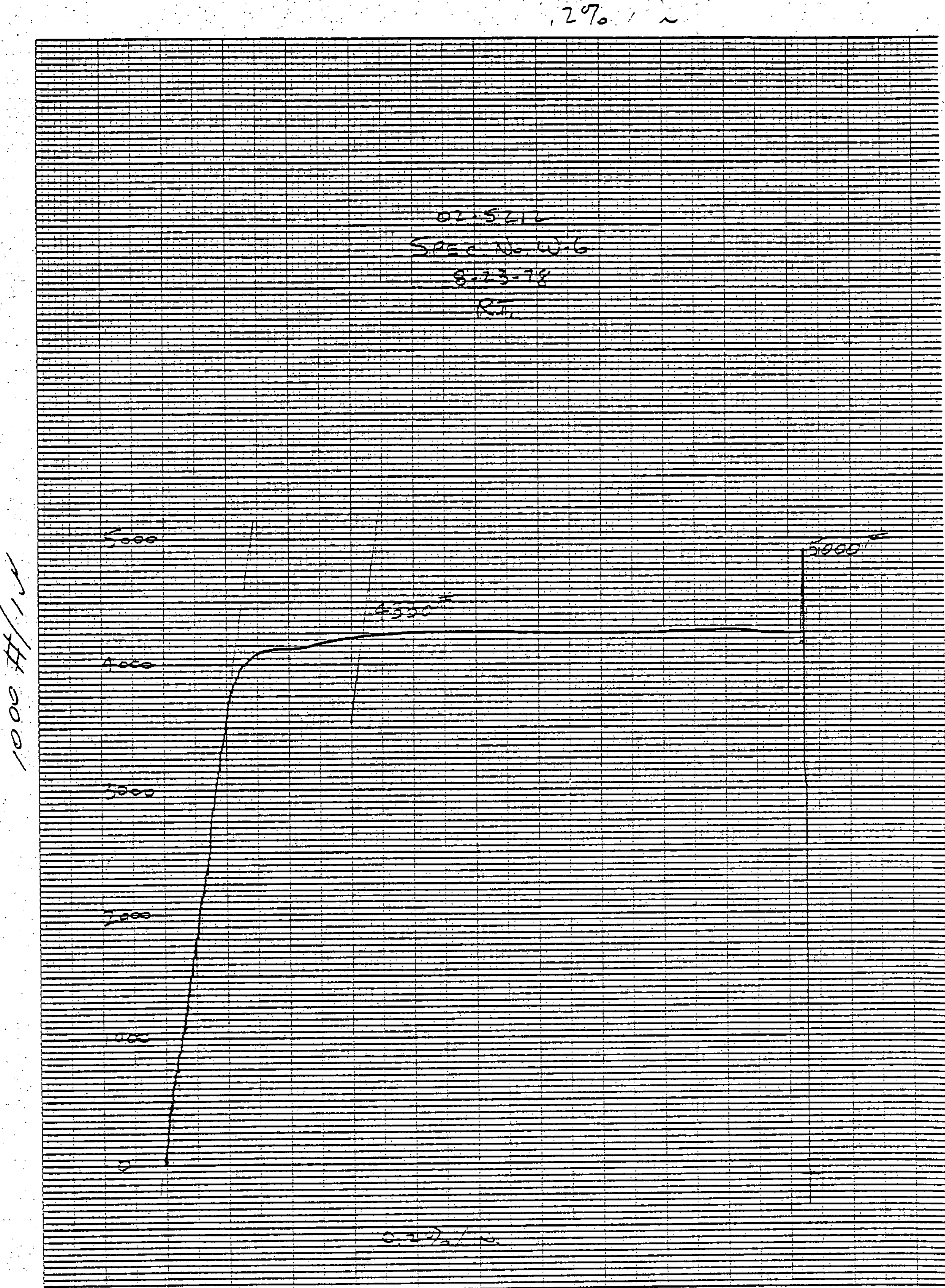

47 1323
K·E 10 X 10 TO ½ INCH • 10 X 15 INCHES
KEUFFEL & ESSER CO. MADE IN U.S.A.

APPENDIX B

PROCEDURE FOR THE GENERATION OF ALLOWABLE PRESSURE-TEMPERATURE LIMIT CURVES FOR NUCLEAR POWER PLANT REACTOR VESSELS

PROCEDURE FOR THE GENERATION OF ALLOWABLE PRESSURE-TEMPERATURE LIMIT CURVES FOR NUCLEAR POWER PLANT REACTOR VESSELS

A. Introduction

The following is a description of the basis for the generation of pressure-temperature limit curves for inservice leak and hydrostatic tests, heatup and cooldown operations, and core operation of reactor pressure vessels. The safety margins employed in these procedures equal or exceed those recommended in the ASME Boiler and Pressure Vessel Code, Section III, Appendix G, "Protection Against Nonductile Failure."

B. Background

The basic parameter used to determine safe vessel operational conditions is the stress intensity factor, K_I, which is a function of the stress state and flaw configuration. The K_I corresponding to membrane tension is given by

$$K_{Im} = M_m \cdot \sigma_m \tag{1}$$

where M_m is the membrane stress correction factor for the postulated flaw and σ_m the membrane stress. Likewise, K_I corresponding to bending is given by

$$K_{Ib} = M_b \cdot \sigma_b \tag{2}$$

where M_b is the bending stress correction factor and σ_b is the bending stress. For vessel section thickness of 4 to 12 inches, the maximum postulated surface flaw, which is assumed to be normal to the direction of maximum stress, has a depth of 0.25 of the section thickness and a length of 1.50 times the section thickness. Curves for M_m versus the square root of the vessel wall thickness for the postulated flaw are given in Figure 1 as taken from the Pressure Vessel Code (ref. Figure G-2114.1). These curves are a function of the stress ratio parameter σ/σ_y, where σ_y is the material yield strength which is taken to be 50,000 psi. The bending correction factor is defined as 2/3 M_m and is therefore determined from Figure 1 as well. The basis for these curves is given in ASME Boiler and Pressure Vessel Code, Section XI, "Rules for Inservice Inspection of Nuclear Power Plant Components," Article A-3000.

The Code specifies the minimum K_I that can cause failure as a function of material temperature, T, and its reference nil ductility temperature, RT_{NDT}. This minimum K_I is defined as the reference stress intensity factor, K_{IR}, and is given by

$$K_{IR} = 26777. + 1223. \exp\left[0.014493(T - RT_{NDT} + 160)\right] \qquad (3)$$

where all temperatures are in degrees Fahrenheit. A plot of this expression is given in Figure 2 taken from the Code (ref. Figure G-2010.1).

C. <u>Pressure-Temperature Relationships</u>

1. <u>Inservice Leak and Hydrostatic Test</u>

During performance of inservice leak and hydrostatic tests, the reference stress intensity factor, K_{IR}, must always be greater than

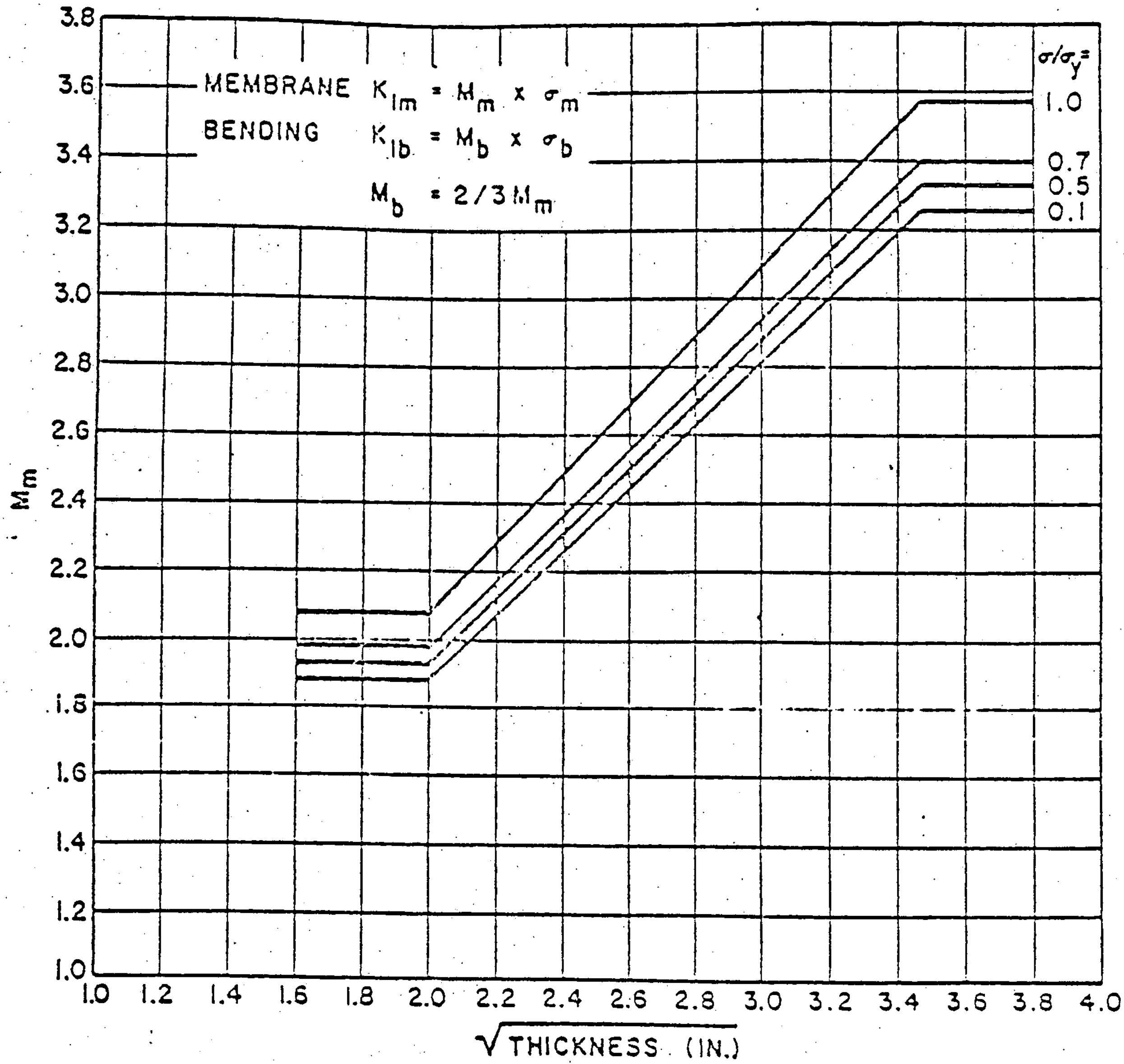

FIGURE 1. STRESS CORRECTION FACTOR

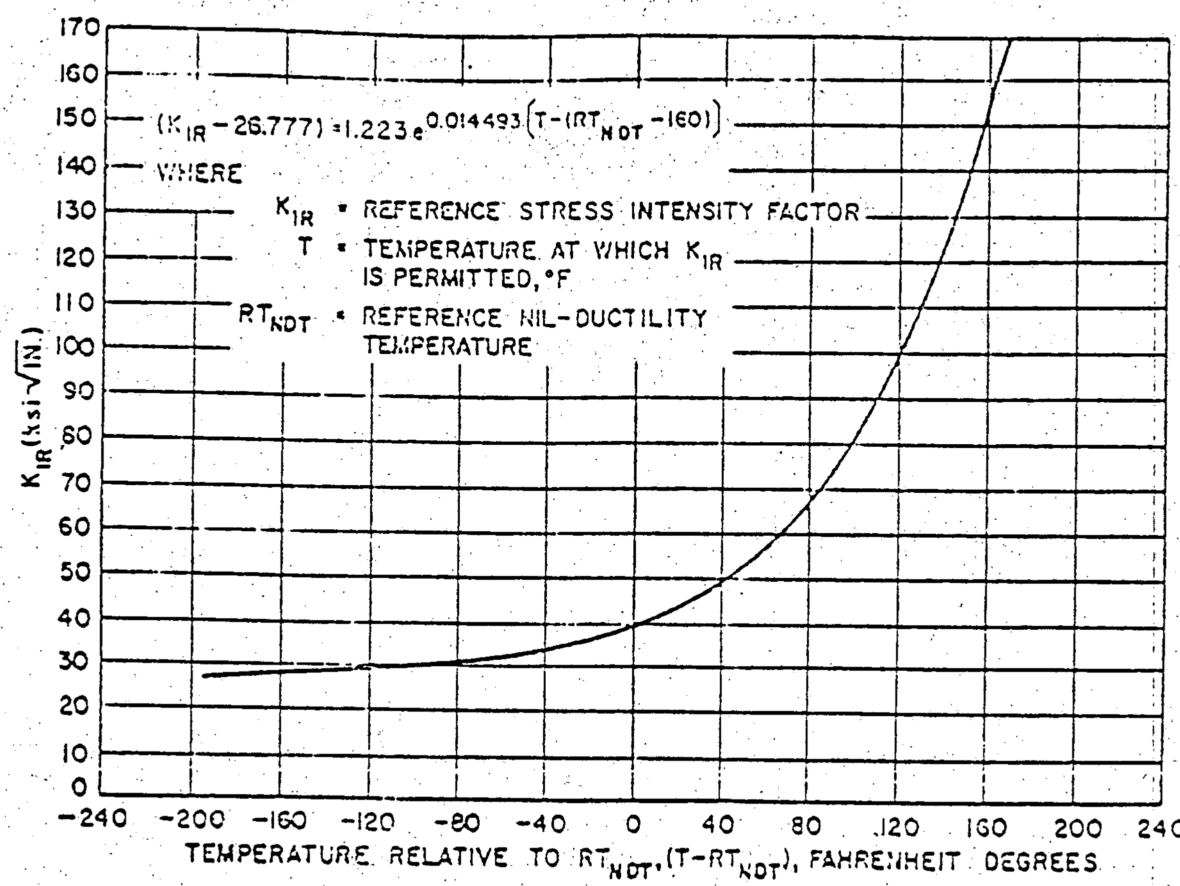

FIGURE 2. REFERENCE STRESS INTENSITY FACTOR

1.5 times the K_I caused by pressure, thus

$$1.5\ K_{Ip} < K_{IR} \tag{4}$$

or

$$1.5\ M_m\ \sigma_m < K_{IR}\ . \tag{5}$$

For a cylinder with inner radius r_i and outer radius r_o, the stress distribution due to internal pressure is given by

$$\sigma(r) = \left(\frac{r_i^2}{r_o^2 - r_i^2}\right)\left(\frac{r_o^2 + r^2}{r^2}\right)\ . \tag{6}$$

With 1/4T flaws possible at both inner and outer radial locations, i.e., at $r_{1/4} = r_i + 1/4(r_o - r_i)$ and $r_{3/4} = r_i + 3/4(r_o - r_i)$, the maximum stress will occur at the inner flaw location, thus

$$\sigma_{max} = P_o\left(\frac{r_i^2}{r_o^2 - r_i^2}\right)\left[\frac{r_o^2 + (1/4r_o + 3/4r_i)^2}{(1/4r_o + 3/4r_i)^2}\right]\ . \tag{7}$$

With the operation pressure known, i.e., P_o, we determine the minimum coolant temperature that will satisfy Equation (4) by evaluating

$$K_{IR} = 1.5\ M_m\ \sigma_{max} \tag{8}$$

and determine the corresponding coolant temperature, T, from Equation (3) for the given RT_{NDT} at the 1/4T location. For this calculation, Equation (3) takes the form

$$T = RT_{NDT}(1/4T) - 160. + 68.9988\ \ln\left[\frac{K_{IR} - 26777.}{1223.}\right]\ . \tag{9}$$

The inservice curves are generated for an operating pressure range of .96 P_o to 1.14 P_o, where P_o is the design operating pressure.

2. Heatup and Cooldown Operations

At all times during heatup and cooldown operations, the reference stress intensity factor, K_{IR}, must always be greater than the sum of 2 times the K_{Ip} caused by pressure and the K_{It} caused by thermal gradients, thus

$$2.0\, K_{Ip} + 1.0\, K_{It} < K_{IR} \tag{10}$$

or

$$2.0\, M_m\, \sigma_{max} = K_{IR} - K_{It} \tag{11}$$

where σ_{max} is the maximum allowable stress due to internal pressure, and K_{It} is the equivalent linear stress intensity factor produced by the thermal gradients. To obtain the equivalent linear stress intensity factor due to thermal gradients requires a detailed thermal stress analysis. The details of the required analysis are given in Section D.

During heatup the radial stress distributions due to internal pressure and thermal gradients are shown schematically in Figure 3a. Assuming a possible flaw at the 1/4T location, we see from Figure 3a that the thermal stress tends to alleviate the pressure stress at this point in the vessel wall and, therefore, the steady state pressure stress would represent the maximum stress condition at the 1/4T location. At

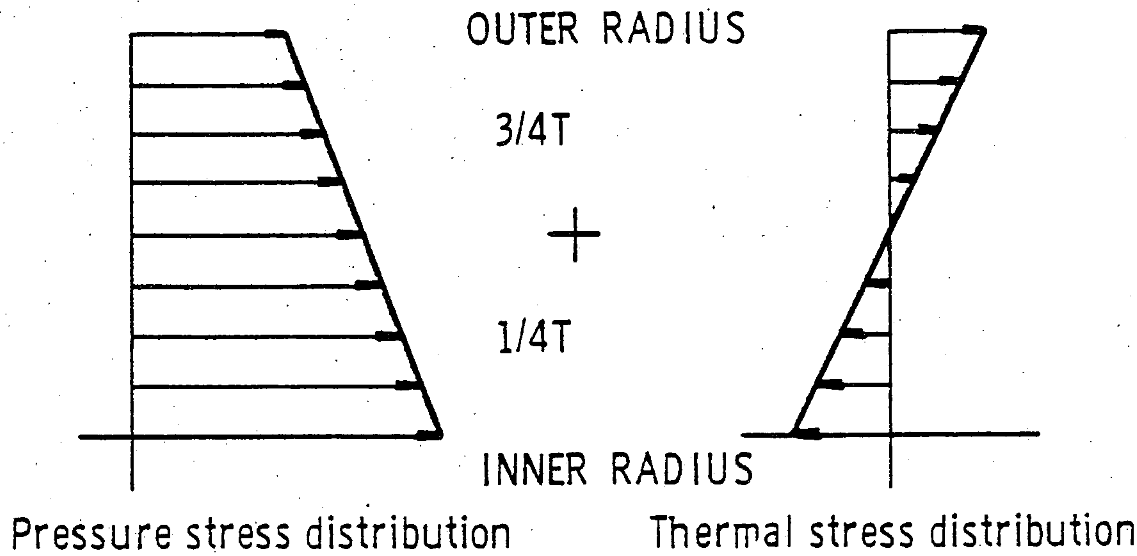

(a) Heatup

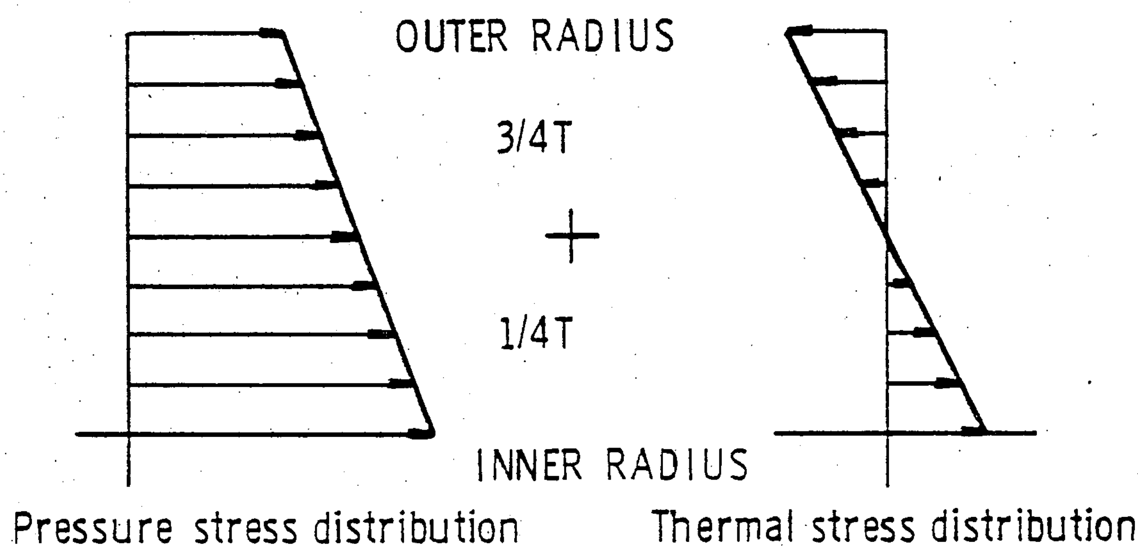

(b) Cooldown

Figure 3. Heatup and Cooldown Stress Distribution

the 3/4T flaw location, the pressure stress and thermal stress add and, therefore, the combination for a given heatup rate represents the maximum stress at the 3/4T location. The maximum overall stress between the 1/4T and 3/4T location then determines the maximum allowable reactor pressure at the given coolant temperature.

The heatup pressure-temperature curves are thus generated by calculating the maximum steady state pressure based on a possible flaw at the 1/4T location from

$$P_{max}(1/4T) = \frac{K_{IR}}{2M_m\left(\frac{r_i^2}{r_o^2 - r_i^2}\right)\left(\frac{r_o^2 + (1/4r_o + 3/4r_i)^2}{(1/4r_o + 3/4r_i)^2}\right)} \qquad (12)$$

where M_m is determined from the curves in Figure 1 and K_{IR} is obtained from Equation (3) using the coolant temperature and RT_{NDT} at the 1/4T location. Here we may note that M_m must be iterated for since it is a function of the final stress ratio to yield strength (σ/σ_y).

At the 3/4T location, the maximum pressure is determined from Equation (11) as

$$P_{max}(3/4T) = \frac{K_{IR} - K_{It}}{2M_m\left(\frac{r_i^2}{r_o^2 - r_i^2}\right)\left(\frac{r_o^2 + (1/4r_i + 3/4r_o)^2}{(1/4r_i + 3/4r_o)^2}\right)} \qquad (13)$$

where K_{IR} is obtained from Equation (2) using the material temperature and RT_{NDT} at the 3/4T location and K_{It} is determined from the analysis procedure outlined in Section D. M_m is determined from Figure 1.

The minimum of these maximum allowable pressures at the given coolant temperature determines the maximum operation pressure. Each heatup rate of interest must be analyzed on an individual basis.

The cooldown analysis proceeds in a similar fashion as that described for heatup with the following exceptions: We note from Figure 3b that during cooldown the 1/4T location always controls the maximum stress since the thermal gradient produces tensile stresses at the 1/4T location. Thus the steady state pressure is the same as that given in Equation (12). For each cooldown rate, the maximum pressure is evaluated at the 1/4T location from

$$P_{max}(1/4T) = \frac{K_{IR} - K_{It}}{2M_m \left(\frac{r_i^2}{r_o^2 - r_i^2}\right)\left(\frac{r_o^2 + (3/4r_i + 1/4r_o)^2}{(3/4r_i + 1/4r_o)}\right)} \qquad (14)$$

where K_{IR} is obtained from Equation (3) using the material temperature and RT_{NDT} at the 1/4T location. K_{It} is determined from the thermal analysis described in Section D.

It is of interest to note that during cooldown the material temperature will lag the coolant temperature and, therefore, the steady state pressure, which is evaluated at the coolant temperature, will initially yield the lower maximum allowable pressure. When the thermal gradients increase, the stresses do likewise, and, finally, the transient analysis governs the maximum allowable pressure. Hence a point-by-point comparison must be made between the maximum allowable pressures produced by steady state analyses and transient thermal analysis to determine the minimum of the maximum allowable pressures.

3. Core Operation

At all times that the reactor core is critical, the temperature must be higher than that required for inservice hydrostatic testing, and in addition, the pressure-temperature relationship shall provide at least a 40°F margin over that required for heatup and cooldown operations. Thus the pressure-temperature limit curves for core operation may be constructed directly from the inservice leak and hydrostatic test and heatup analysis results.

D. Thermal Stress Analysis

The equivalent linear stress due to thermal gradients is obtained from a detailed thermal analysis of the vessel. The temperature distribution in the vessel wall is governed by the partial differential equation

$$\rho c T_t - K\left[(1/r)\,T_r + T_{rr}\right] = 0 \tag{15}$$

subject to initial condition

$$T(r, 0) = T_o \; , \tag{16}$$

and boundary conditions

$$-KT_r(r_i, t) = h\left[T_c(t) - T(r_i, t)\right] , \tag{17}$$

and

$$T_r(r_o, t) = 0 \tag{18}$$

where

$$T_c = T_o + Rt. \tag{19}$$

ρ is the material density, c the material specific heat, K the heat conductivity of the material, h the heat transfer coefficient between the water coolant and vessel material, R the heating rate, T_o the initial coolant temperature, $T(r,t)$ the temperature distribution in the vessel, r the spatial coordinate, and t the temporal coordinate.

A finite difference solution procedure is employed to solve for the radial temperature distribution at various time steps along the heatup or cooldown cycle. The finite difference equations for N radial points, at distance Δr apart, across the vessel are:

for $1 < n < N$

$$T_n^{t+\Delta t} = \left[1 - \frac{\Delta t K}{\rho c(\Delta r)^2}\left(2 + \frac{\Delta r}{r_n}\right)\right] T_n^t + \frac{\Delta t K}{\rho c(\Delta r)^2}\left[\left(1 + \frac{\Delta r}{r_n}\right) T_{n+1}^t + T_{n-1}^t\right], \tag{20}$$

for $n = 1$

$$T_1^{t+\Delta t} = \left[1 - \frac{\Delta t K}{\rho c(\Delta r)^2}\left(1 + \frac{\Delta r}{r_1}\right) - \frac{\Delta t h}{\rho c(\Delta r)}\right] T_1^t + \frac{\Delta t K}{\rho c(\Delta r)^2}\left[\left(1 + \frac{\Delta r}{r_1}\right) T_2^t + \frac{\Delta r h}{K} T_c^t\right], \tag{21}$$

and for $n = N$

$$T_N^{t+\Delta t} = \left[1 - \frac{\Delta t\, K}{\rho c (\Delta r)^2}\right] T_N^t + \frac{K \Delta t}{\rho c (\Delta r)^2} T_{N-1}^t \quad . \tag{22}$$

For stability in the finite difference operation, we must choose Δt for a given Δr such that both

$$\frac{\Delta t\, K}{\rho c (\Delta r)^2}\left(2 + \frac{\Delta r}{r_1}\right) \leq 1 \tag{23}$$

and

$$\frac{\Delta t\, K}{\rho c (\Delta r)^2}\left(1 + \frac{\Delta r}{r_1}\right) + \frac{\Delta t\, h}{\rho c (\Delta r)} \leq 1 \tag{24}$$

are satisfied. These conditions assure us that heat will not flow in the direction of increasing temperature, which, of course, would violate the second law of thermodynamics.

Since a large variation in coolant temperature is considered, the dependence of $(K/\rho c)$, K, and h on temperature is included in the analysis by treating these as constants only during every 5°F increment in coolant temperature and then updating their values for the next 5°F increment. The dependence of $(K/\rho c)$ called the thermal diffusivity and K, the thermal conductivity, can be determined from the ASME Boiler and Pressure Vessel Code, Section III, Appendix I - Stress Tables. A linear regression analysis of the tabular values resulted in the following expressions:

$$K(T) = 38.211 - 0.01673 * T \text{ (BTU/HR-FT-°F)} \tag{25}$$

and

$$k(T) = (K/\rho c) = 0.6942 - 0.000432 * T \; (FT^2/HR) \tag{26}$$

where T is in degrees Fahrenheit.

The heat transfer coefficient is calculated based on forced convection under turbulent flow conditions. The variables involved are the mean velocity of the fluid coolant, the equivalent (hydraulic) diameter of the coolant channel, and the density, heat capacity, viscosity, and thermal conductivity of the coolant. For water coolant, allowance for the variations in physical properties with temperature may be made by writing*

$$h(T) = 170\,(1 + 10^{-2} * T - 10^{-5} * T^2)\, v^{0.8}/D^{0.2} \tag{27}$$

where v is in ft/sec, D in inches, the temperature is in °F, and h is in Btu/hr-ft^2-°F. The values for the heat-transfer coefficient given by this relationship are in good agreement with those obtained from the Dittus-Boelter equation for temperatures up to 600°F. The mean velocity of the coolant, v, is generally given in terms of the effective coolant flow rate Q (Lbm/hr) and effective flow area A (ft^2). Given the relationship

$$\rho(T) = 62.93 - 0.48 \times 10^{-2} * T - 0.46 \times 10^{-4} * T^2 \tag{28}$$

for the density of water as a function of temperature, the mean velocity of the coolant is obtained from

$$v = Q/(3600 * \rho(T) * A) \;. \tag{29}$$

---

* Glasstone, S., Principles of Nuclear Reactor Engineering, D. Van Nostrand Co., Inc., New Jersey, pp. 667-668, 1960.

The thermal stress distribution is calculated from

$$\sigma_T(r,t) = \frac{\alpha E}{1-\nu}\left[\frac{1}{r^2}\int_{r_i}^{r} T(r,t)\,r\,dr - T(r,t) + \frac{1}{r^2}\left(\frac{r^2+r_i^2}{r_o^2-r_i^2}\right)\int_{r_i}^{r_o} T(r,t)\,r\,dr\right] \qquad (30)$$

where α is the coefficient of thermal expansion (in/in °F), E is Young's modulus, and ν is Poisson's ratio. This expression can be obtained from Theory of Elasticity by Timoshenko and Goodier, pp. 408-409, when imposing a zero radial stress condition at the cylinder inner and outer radius. Poisson's ratio is taken to be constant at a value of 0.3 while α and E are evaluated as a function of the average temperature across the vessel

$$T_{avg} = \frac{2}{(r_o^2 - r_i^2)}\int_{r_i}^{r_o} T(r)\,r\,dr \; . \qquad (31)$$

The dependence of the coefficient of thermal expansion on temperature is taken to be

$$\alpha(T) = 5.76 \times 10^{-6} + 4.4 \times 10^{-9} * T \qquad (32)$$

and the dependence of Young's modulus on temperature is taken to be

$$E(T) = 27.9142 + 2.5782 \times 10^{-4} * T - 6.5723 \times 10^{-6} * T^2 \qquad (33)$$

as obtained from regression analysis of tabular values given in Section III, Appendix I of the ASME Boiler and Pressure Vessel Code.

The resulting stress distribution given by Equation (30) is not linear; however, an equivalent linear stress distribution is determined from the resulting moment. The moment produced by the nonlinear stress distribution is given by

$$M(t) = b\int_{r_i}^{r_o} \sigma_T(r,t)\, r\, dr \tag{34}$$

where b is a unit depth of the vessel. Here we note that the moment is a function of time, i.e., coolant temperature via $T_c = To + Rt$. For a linear stress distribution we have that

$$\sigma_{max} = \frac{Mc}{I} \tag{35}$$

where σ_{max} is the maximum outer fiber stress, c the distance from the neutral axis, taken to be $(r_o - r_i)/2$, and I the section area moment of inertia which is given by

$$I = \frac{bh^3}{12} = \frac{b(r_o - r_i)^3}{12} \quad . \tag{36}$$

Combining these expressions results in the equivalent linear stress due to thermal gradients

$$\sigma_{max} = \sigma_{bt} = \frac{6}{(r_o - r_i)^2}\int_{r_i}^{r_o} \sigma_T(r,t)\, r\, dr \tag{37}$$

The thermal stress intensity factor K_{It} is then defined as

$$K_{It} = M_b\, \sigma_{bt} \tag{38}$$

where M_b is determined from the curves given in Figure 1 wherein $M_b = 2/3\ M_m$. It is of interest to note that a sign change occurs in the stress calculations during a cooldown analysis since the thermal gradients produce compressive stresses at the vessel outer radius. This sign change must then be reflected in the K_{It} calculation for the cooldown analysis.

Normalized temperature and thermal stress distributions during a typical reactor heatup are given in Figure 4. The radial temperature is shown normalized with respect to the average temperature, T_{avg}, by

$$T = \frac{T - T_{avg}}{(T - T_{avg})_{max}} \quad . \tag{39}$$

The thermal stress and equivalent linearized stress, as calculated by Equations (30) and (37), are normalized with respect to the maximum thermal stress. Here we note that the actual thermal stress at the 3/4T location is considerably less than the maximum equivalent linear stress which yields additional safety margins during the heatup cycle. Similar temperature and thermal stress distributions are developed during cooldown. The trends are nearly identical as those shown in Figure 4 when the inner and outer vessel locations are reversed with the 1/4T location becoming the critical point.

E. Example Calculations

The following example is based on a reactor vessel with the following characteristics:

Inner Radius	=	82.00 in.	(r_i)
Outer Radius	=	90.00 in.	(r_o)
Operating Pressure	=	2250 psig	(P_o)

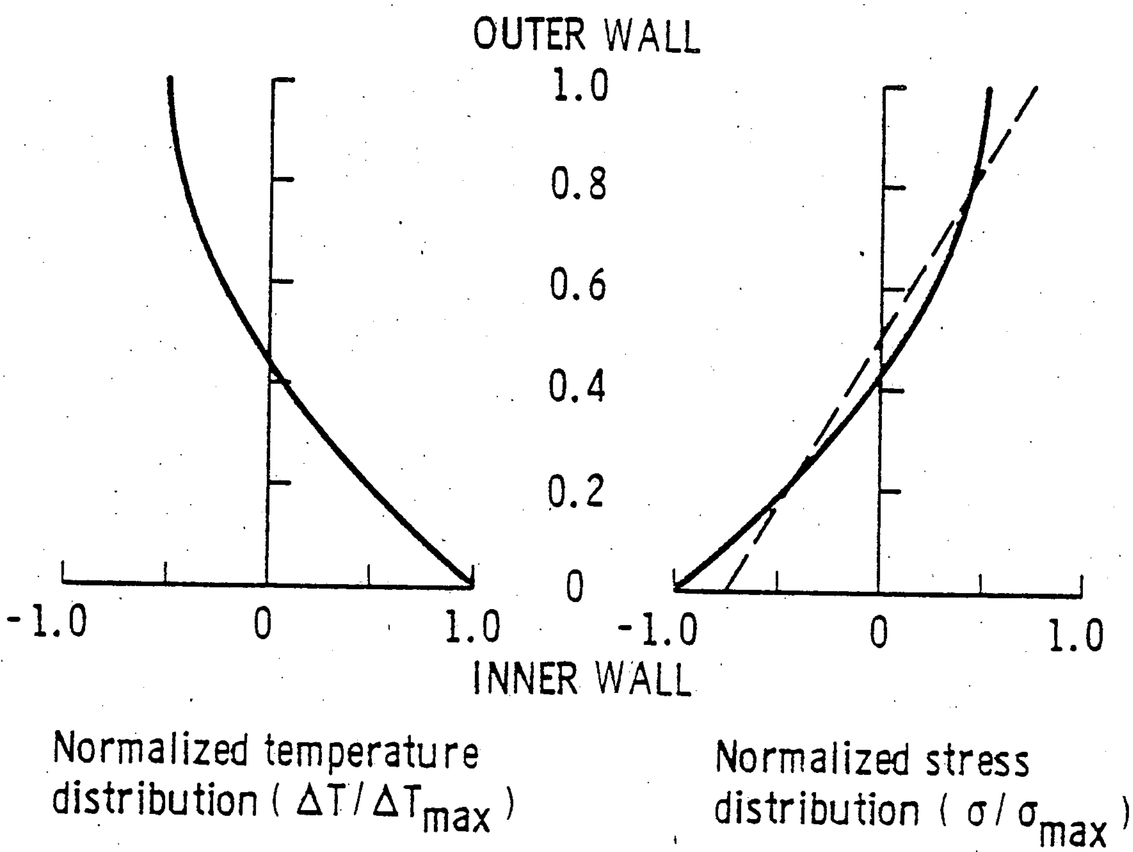

Figure 4. Typical Normalized Temperature and Stress Distribution During Heatup

Initial Temperature	=	70°F	(T_o)
Final Temperature	=	550°F	(T_f)
Effective Coolant Flow Rate	=	100×10^6 Lbm/hr	(Q)
Effective Flow Area	=	20.00 ft^2	(A)
Effective Hydraulic Diameter	=	10.00 in.	(D)
RT_{NDT} (1/4T)	=	200°F	
RT_{NDT} (3/4T)	=	140°F	

In the thermal stress analysis 21 radial points were used in the finite difference scheme. Going from 70°F to the final temperature of 550°F, approximately 12,000 time (temperature via $T = To + Rt$) steps were required in the thermal analysis for the 100°F/hr heatup rate. The results of the computation are shown in Figures 5 through 9.

Figure 5 gives the reference stress intensity factor, K_{IR}, as a function of temperature indexed to RT_{NDT} (1/4T). For the steady state analysis, K_{IR} is converted directly to allowable pressure via Equation 12.

During the heatup and cooldown thermal analyses the material temperature at the 1/4T and 3/4T and thermal stress intensity factors K_{It} are required to compute allowable pressure via Equations (13) and (14). The material temperatures versus coolant temperature during the 100°F/hr heatup and cooldown analyses are given in Figure 6. These temperatures allow computation of the corresponding reference stress intensity factors, K_{IR} (3/4T) and K_{IR} (1/4T). Figure 7 gives the corresponding thermal stress intensity factor at the 3/4T and 1/4T locations as a function of coolant temperature.

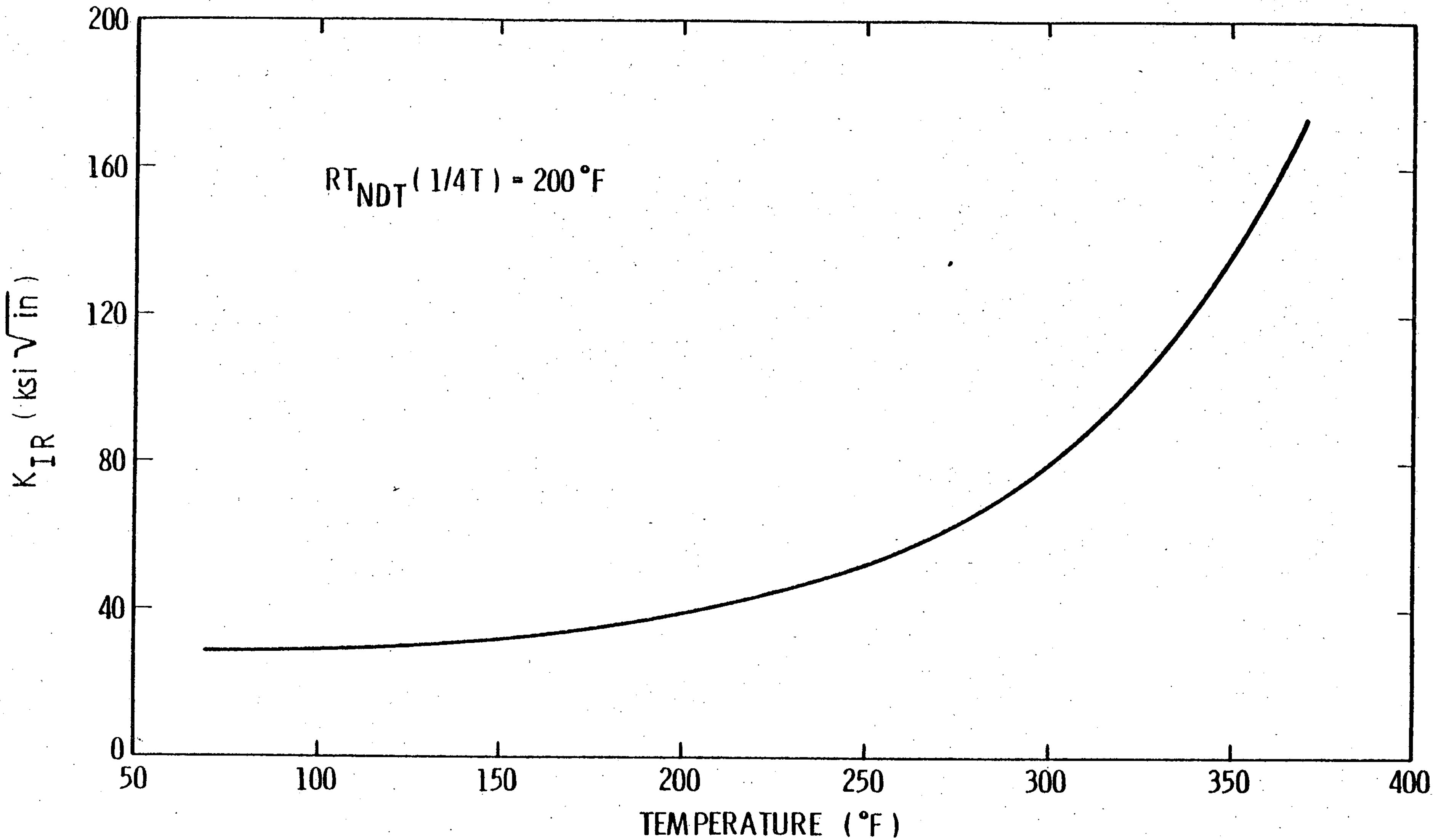

Figure 5. Reference Stress Intensity Factor as a Function of Temperature Indexed to RT_{NDT} (1/4T)

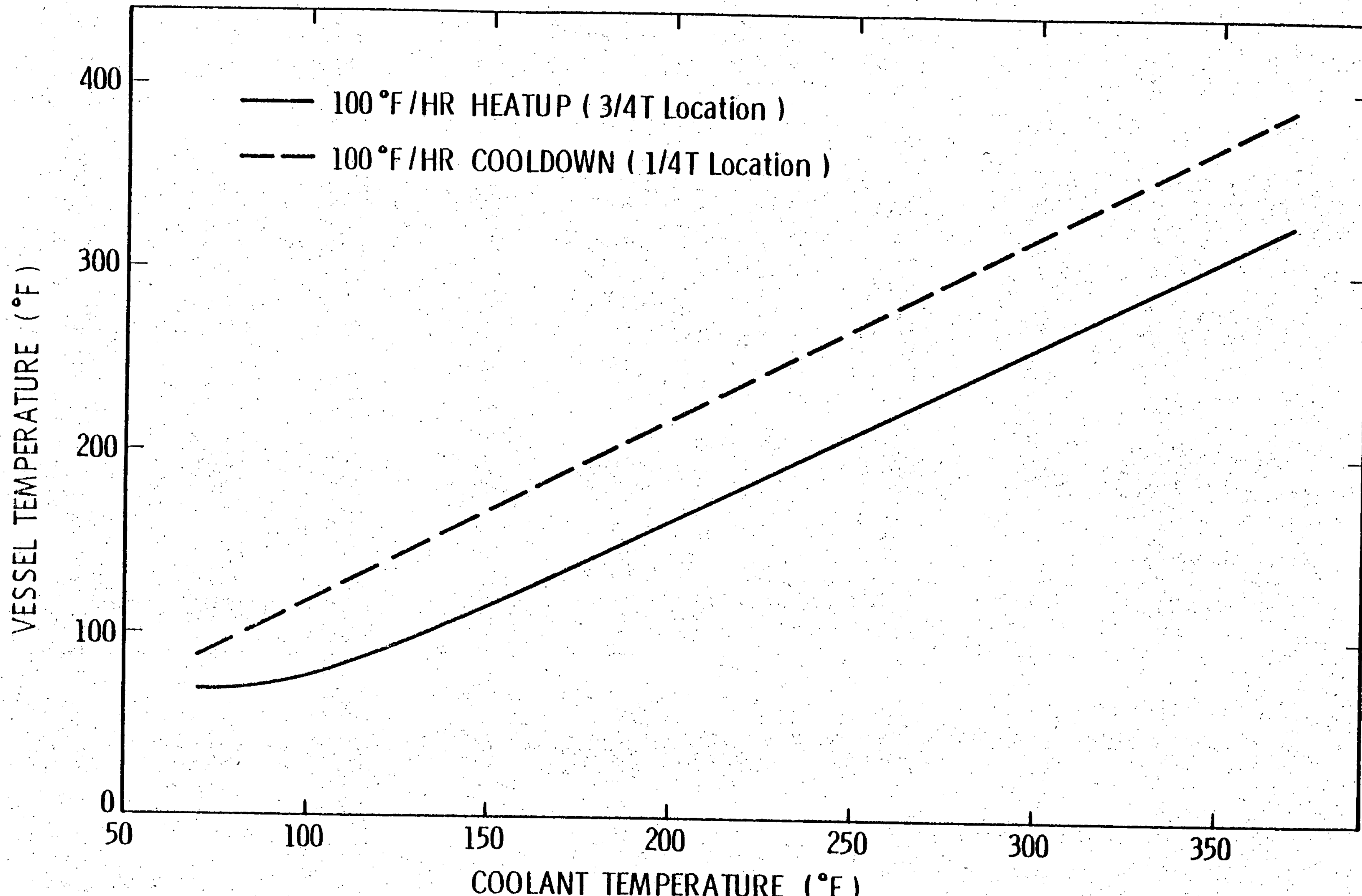

Figure 6. Vessel Temperature at 1/4T and 3/4T Locations as a Function of Coolant Temperature

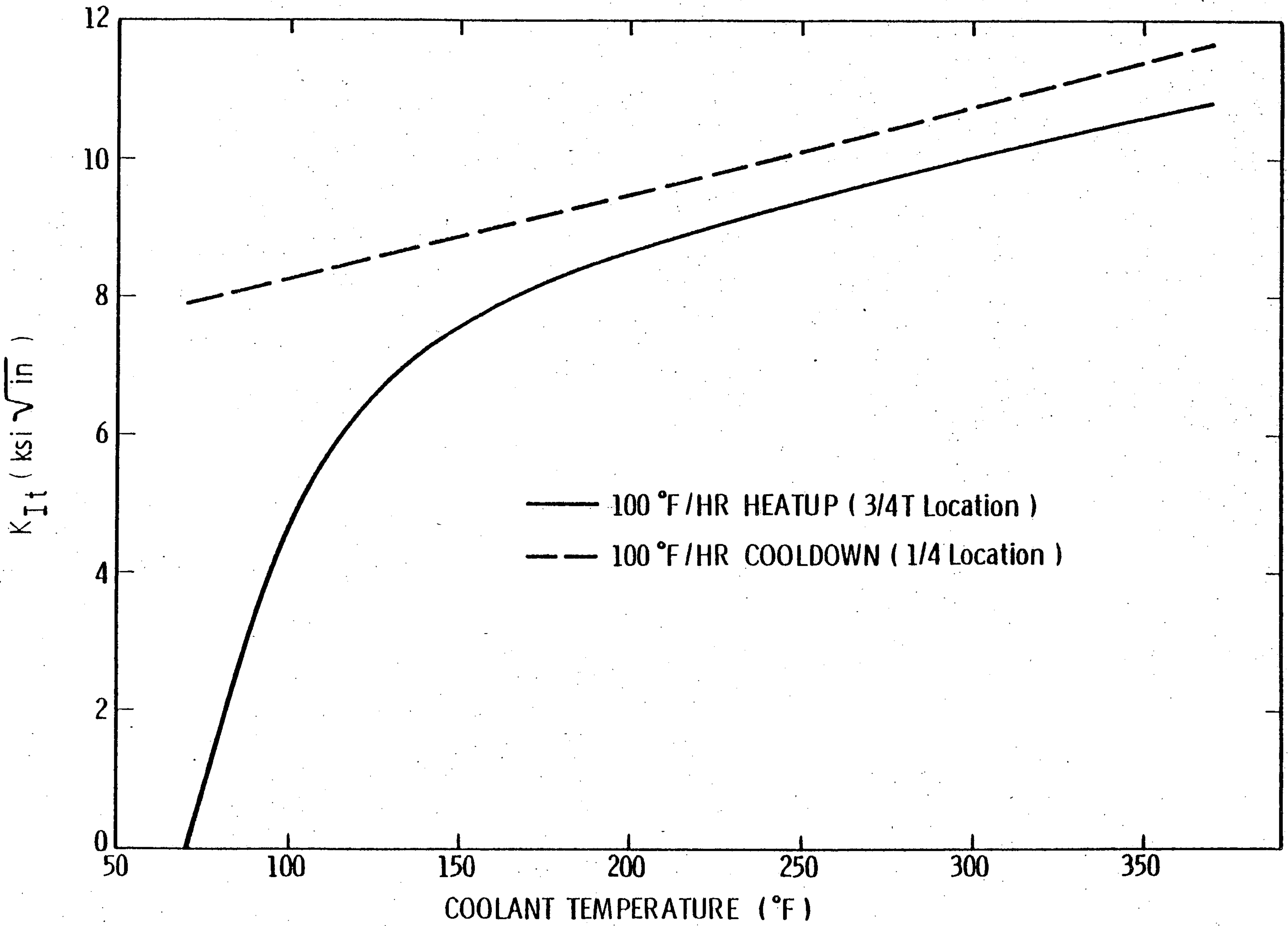

Figure 7. Thermal Stress Intensity Factor at 3/4T and 1/4T Locations as a Function of Coolant Temperature

Figures 8 and 9 demonstrate the construction of the allowable composite pressure and temperature curves for the 100°F/hr heatup and cooldown rates. The composite curves represent the lower bound of the thermal and steady state curves with the addition of margins of +10°F and -60 psig for possible instrumentation error. Figure 8 also shows the leak test limit, corrected for instrument error, as obtained from Equation (9). The limit points are at the operating pressure 2250 psig and at 2475 psig which corresponds to 1.1 times the operating pressure. The criticality limit is also shown in Figure 8 and is constructed by providing for a 40°F margin over that required for heatup and cooldown and by requiring that the minimum temperature be greater than that required by the leak test limit.

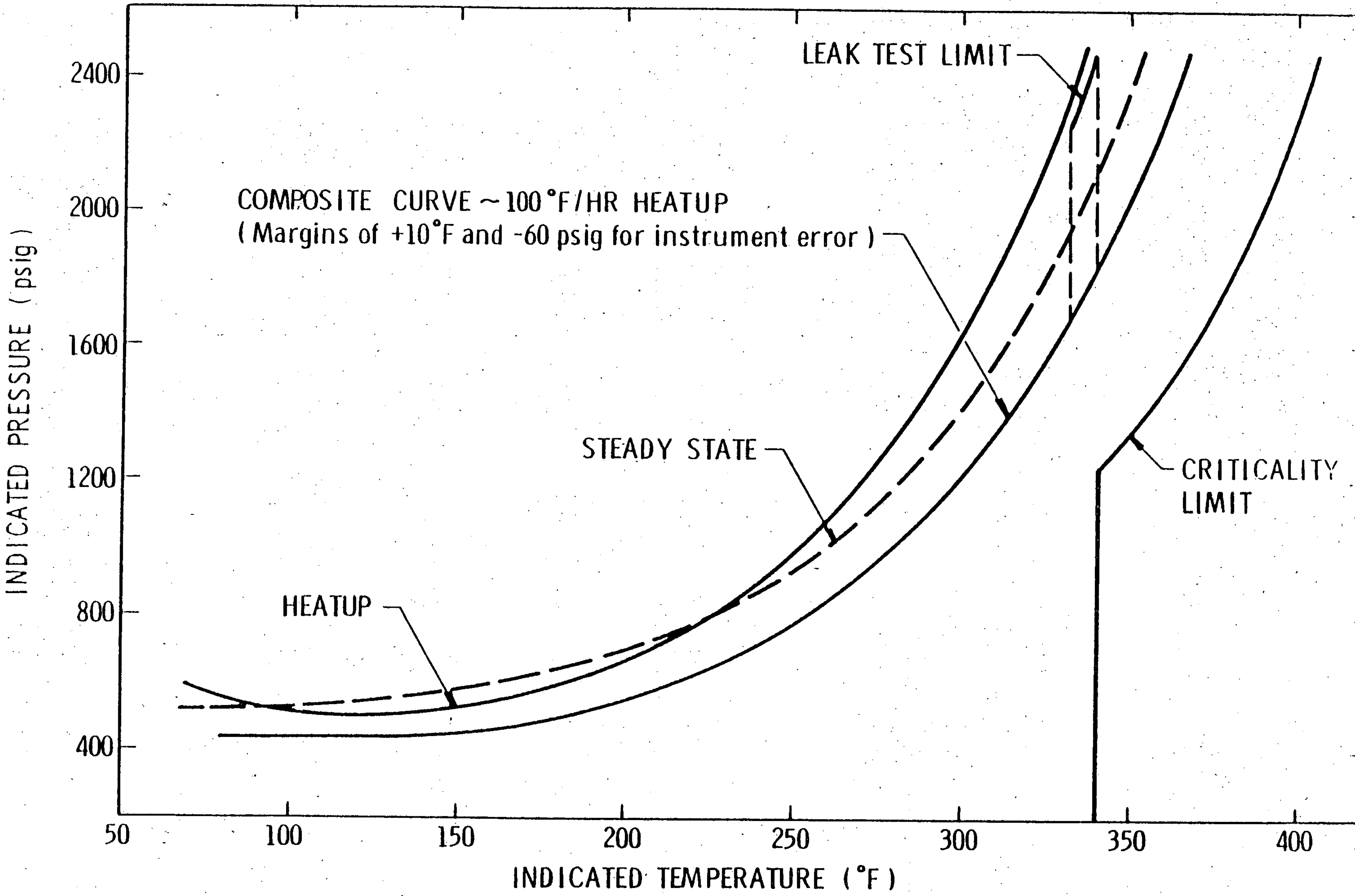

Figure 8. Pressure - Temperature Curves for 100°F/Hr Heatup

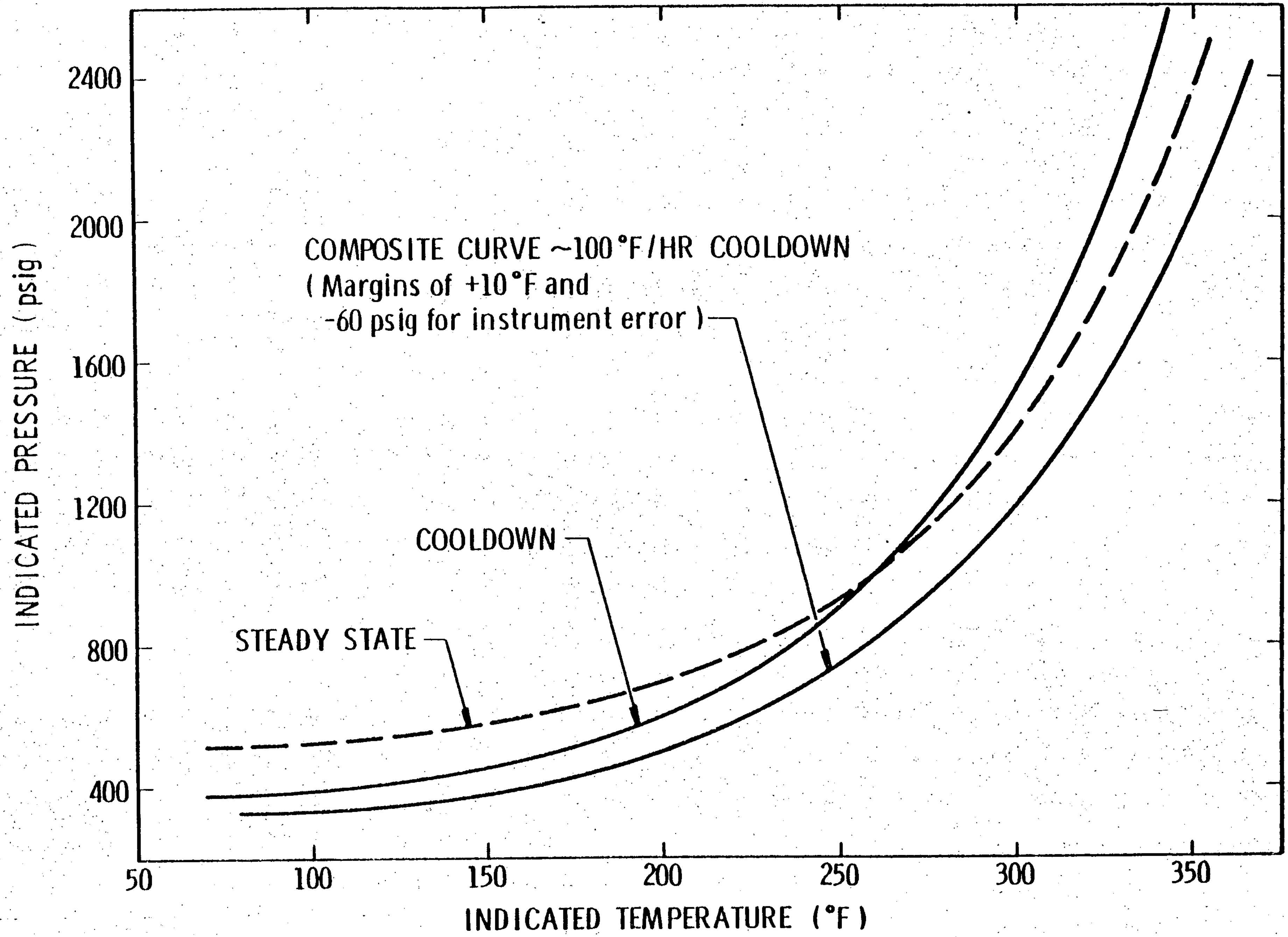

Figure 9. Pressure-Temperature Curves for 100°F/Hr Cooldown